

**NATIONAL ACADEMY OF SCIENCES
NATIONAL RESEARCH COUNCIL
of the
United States of America**

**UNITED STATES NATIONAL COMMITTEE
International Scientific Radio Union**



**1968 FALL MEETING
10-12 September**

**Jointly Sponsored by
Six Groups of the Institute of
Electrical and Electronics Engineers
and also by
The American Meteorological Society**

**NORTHEASTERN UNIVERSITY
Boston, Massachusetts**

Price \$2.00

MEETING SCHEDULE

date time

Monday 1930
9 September

U.S. NATIONAL COMMITTEE MEETING

455EC

Tuesday 0800 Registration – Hotel Somerset (Northeastern University other times)

10 September

0900 URSI/G-AP – COMBINED SESSION (Somerset)

Session designation–Scheduled No. of Papers – Room No. – Page in Digest

COMMISSION

		I	page	II		page	III		page	IV		page	VI		page
	1400			2.1-8	109RB	15	3.1-8	107RB	41				6.1-6	455EC	75
Wednesday	0900			2/6-7	356EC	21	3/4-8	107RB	47	4/3-8	107RB	47	6/2-7	356EC	21
11 September							3.2-8	109RB	52						
	1300	BS	349EC												
	1400			2.2-6	109RB	26	3.3-8	107RB	56				6.2-7	455EC	81
	1700			BS	109RB										
	1730						BS	107RB					BS	455EC	
Thursday	0900	1/6-6	455EC	3	2.3-5	355EC*	32	3.4-8	356EC	62			6.3-6	107RB	88
12 September													6.4-7	109RB	93
	1400	1.1-8	455EC	7	2.4-7	355EC*	35	3.5-6	356EC	66			6/1-6	455EC	3

NOTES: ROOMS

107, 109 RB are in Robinson Hall (#23 map)

355, 356, 455EC are on the E11 Student Center (#21 Map)

TRANSPORTATION

A shuttle bus is to be provided during session hours between Northeastern and the Somerset Hotel.

BS

Business Session

*These sessions are being held in conjunction with the AMS

1930 Monday. 9 Sept.

Room 455EC

USA NATIONAL COMMITTEE MEETING

0900 - 1230 Tuesday. 10 Sept.

Somerset Hotel

JOINT URSI/GAP TECHNICAL SESSION

The areas of interest of the International Scientific Radio Union and of the IEEE group on Antennas and Propagation cover a wide spectrum of technical topics. Rather than select several papers from each organization for the combined technical session, it was decided to have a series of invited papers on subjects of interest to both groups. The program is as follows.

ELECTROMAGNETIC WAVES -- A TOOL FOR SENSING AND EXPLORATION

MODERATOR: WILLIAM E. GORDON, RICE UNIVERSITY

1. WELCOMING REMARKS, Asa S. Knowles, President, Northeastern University
2. RADAR AS A SENSOR OF THE EARTH'S SURFACE, Prof. Richard K. Moore, University of Kansas.
3. ELECTROMAGNETIC WAVES IN NONLINEAR OPTICAL MEDIA, Prof. Nicolaas Bloembergen Harvard University.
4. BISTATIC RADAR STUDIES OF PLANETARY ATMOSPHERES AND SURFACES, Prof. Von R. Eshleman, Stanford University.
5. ELECTROMAGNETIC WAVES (LASERS) FOR BIOLOGICAL AND MEDICAL APPLICATIONS, Prof. Samuel Fine, Northeastern University.

BANQUET

The combined URSI/G-AP Banquet will be held Tuesday, 10 September at the Somerset Hotel, 400 Commonwealth Ave. Boston. The banquet will begin at 1900 and will be preceded at 1800 by a no-host cocktail hour.

The Banquet Speaker will be Dr. Harold Edgerton, Institute Professor MIT and Honary Chairman of the Board of E G & G. The title of the talk is UNDERWATER PHOTOGRAPHY and will be illustrated with some of "Doc's" famous pictures.

Banquet tickets should preferably be ordered in advance. Please see the Registration card.

INTERNATIONAL SCIENTIFIC RADIO UNION
U. S. NATIONAL COMMITTEE

- Chairman - Prof. E. C. Jordan (University of Illinois)
Vice-Chairman - Prof. A. T. Waterman, Jr. (Stanford University)
Secretary - Prof. F. S. Johnson (SW Center for Advanced Studies)
Editor - Prof. S. A. Bowhill (University of Illinois)
Immediate Past-Chairman - Prof. M. G. Morgan (Dartmouth College)
- Executive Committee - The foregoing, plus
Prof. H. G. Booker (Univ. of California, San Diego)
Prof. M. Chodrow (Stanford University)
Prof. W. E. Gordon (Rice University)
Prof. S. Silver (Univ. of California, Berkeley)

The National Committee maintains the following technical commissions
Current chairmen and their affiliations are given.

1. Radio Measurement Methods and Standards

Dr. Bruno O. Weinschel
P. O. Box 577
Gaithersburg, Maryland 20760

2. Radio and Non-ionized Media

Dr. D. C. Hogg
Bell Telephone Labs., Inc.
P. O. Box 400
Holmdel, New Jersey 07733

3. On the Ionosphere

Prof. O. G. Villard
Stanford Electronics Labs
Radioscience Laboratory
Stanford, California 94305

4. On the Magnetosphere

Prof. K. L. Bowles
Department of Applied Electrophysics
University of California
P. O. Box 109
La Jolla, California 92037

5. Radio and Radar Astronomy

Prof. W. C. Erickson
Clark Lake Radio Observatory
P. O. Box 73
Borrego Springs, California 92004

6. Radio Waves and Transmission Information

Dr. R. C. Hansen
KMS Industries, Inc.
220 E. Huron Street
Ann Arbor, Michigan 48106

7. Radio Electronics

Prof. Hubert Heffner
Stanford Electronics Laboratory
Stanford University
Stanford, California 94305

OTHER MEMBERS OF THE U. S. A.

NATIONAL COMMITTEE

Members-at-Large:

Dr. C. M. Crain	Prof. J. P. Hagen
Dr. A. J. Dessler	Dr. W. B. Hanson
Dr. J. V. Evans	Mr. W. W. Mumford
Prof. R. G. Fellers	Dr. K. M. Seigel
Dr. J. W. Findlay	Prof. A. W. Straiton
Dr. O. K. Garriott	Dr. T. E. Van Zandt

Institute of Electrical and Electronics Engineers:

Prof. E. Weber

United States Government:

Commerce	Mr. A. H. Shapley
Defense	Mr. E. Paroulek
Air Force	Mr. J. E. Keto
Army	Mr. F. H. Dickson
Navy	Dr. A. H. Schooley
FCC	Mr. H. Fine
NASA	Dr. E. R. Schmerling
NSF	Dr. E. H. Hurlburt
ODTM	Mr. W. E. Plummer

Honorary:

Dr. H. H. Beverage
Prof. A. H. Waynick

Ex-Officio:

Officers of URSI resident in the United States (including honorary presidents, chairmen and vice-chairmen of commissions)

President	Prof. S. Silver
Chairman of Commission IV	Prof. H. G. Booker
Vice-Chairman of Commission II	Prof. W. E. Gordon
Vice-Chairman of Commission VII	Prof. M. Chodorow
Foreign Secretary of National Academy of Sciences	Prof. H. S. Brown
Chairman of Division of Physical Sciences, NAS	Prof. E. L. Goldwasser

DESCRIPTION OF INTERNATIONAL SCIENTIFIC RADIO UNION

The International Scientific Radio Union is one of 14 world scientific unions organized under the International Council of Scientific Unions (ICSU). It is commonly designated as URSI (from its French name, Union Radio Scientifique Internationale). Its aims are (1) to promote the scientific study of radio communications; (2) to aid and organize radio research requiring cooperation on an international scale and to encourage the discussion and publication of the results; and, (3) to facilitate agreement upon common methods of measurement and the standardization of measuring instruments. The International Union itself is an organizational framework to aid in promoting these objectives. The actual technical work is largely done by the National Committees in the various countries.

The officers of the International Union are:

President:	Prof. S. Silver (USA)
Immediate Past President:	Prof. I. Koga (Japan)
Vice Presidents:	Dr. J. Groszkowski (Poland)
	Prof. W. J. G. Beynon (UK)
	Prof. M. Boella (Italy)
	Prof. W. Dieminger (DBR)
Treasurer:	Prof. Ch. Manneback (Belgium)
Acting Secretary General:	Prof. C. M. Minnis (Belgium)
Honorary Presidents:	Mr. B. Decaux (France)
	Dr. R. L. Smith-Rose (UK)
	Mr. J. A. Ratcliffe (UK)

The Secretary's office and the headquarters of the organization are located at 7, Place Emile Danco, Uccle, Brussels 18, Belgium. The Union is supported by contributions (dues) from 37 member countries. Additional funds for symposia and other scientific activities of the Union are provided by ICSU from contributions received for this purpose from UNESCO.

The International Union has seven permanent bodies called "Commissions" for centralizing studies in the principal technical fields. In addition, Commission VIII has been newly established on a provisional basis. The names of the Commissions and the chairmen are as follows:

- I. Radio Standards and Measurements
Dr. L. Essen (United Kingdom)
- II. Radio and Non-ionized Media
Dr. J. A. Saxton (United Kingdom)
- III. On the Ionosphere
Dr. C. O. Hines (Canada)
- IV. On the Magnetosphere
Prof. H. G. Booker (United States)
- V. Radio Astronomy
Dr. E. J. Blum (France)
- VI. Radio Waves and Circuits
Dr. F. L. Stumpers (Netherlands)
- VII. Radio Electronics
Prof. P. A. Grivet (France)
- VIII. On Radio Noise of Terrestrial Origin
Mr. F. Horner (United Kingdom)

Every three years the International Union holds a meeting called the General Assembly. The latest of these, the XV'th, was held in Munich, Germany, in September 1966. The Secretariat prepares and distributes the Proceedings of these General Assemblies. The International Union arranges international symposia on specific subjects pertaining to the work of one Commission or to several Commissions. The International Union also cooperates with other Unions in international symposia on subjects of joint interest.

Radio is unique among the fields of scientific work in having specific adaptability to large-scale international research programs, for many of the phenomena that must be studied are world-wide in extent and yet are in a measure subject to control by experimenters. The new activity in the exploration of space and the extension of our scientific observations to the space environment is dependent on radio for its communication link and at the same time expands the scope of radio research. One of its branches, radio astronomy, involves cosmos-wide phenomena. URSI has in all this a distinct field of usefulness in furnishing a meeting ground for the numerous workers in the manifold aspects of radio research its meetings and committee activities furnish valuable means of promoting research through exchange of ideas.

COMMISSION 1
RADIO MEASUREMENT METHODS AND STANDARDS

Dr. B.O. Weinschel, Chairman

Session	Pages
<i>1/6 ANTENNA MEASUREMENTS (Joint with Commission 6)</i>	
0900 Thursday, 12 September Room 455EC	
Chairman: Dean A.B. Giordano Polytechnic Institute of Brooklyn Route 110 Farmingdale, New York 11735	3-6
<i>1-1 MICROWAVE MEASUREMENTS</i>	
1400 Thursday, 12 September Room 455EC	
Chairman: Dr. H.M. Altschuler ESSA Boulder, Colorado 80301	7-11

Business Meeting Will Be Held From 1300 to 1730, Wednesday, 11 September in Room 349EC.

1300 Wednesday, 11 September

ROOM 349EC

BUSINESS SESSION FOR COMMISSION 1

1

ANTENNA MEASUREMENTS

A.B. Giordano, Chairman

1

1/6-1 DEVELOPMENT OF A SINGLE FIGURE-OF-MERIT FOR D/F SITE EVALUATION.
L. A. Lyons, Research Analysis Corporation, McLean, Virginia 22101

An earlier paper¹ indicated that a single parameter may be employed to evaluate the suitability of many D/F sites. Experiments showed that this parameter can be determined by examining the fluctuations in the power received at a site from a fixed position target transmitter whose frequency is varied over an arbitrary band. In this paper analytical support of this result is given. It is shown that the variance of the electric field in the vicinity of a number of hemispherical bosses on a perfectly conducting horizontal plane illuminated by a vertically polarized plane wave is the same for samples taken either at different angles of arrival of the direct wave or at different frequencies. The conditions under which this is true are: 1) The radii of the bosses lie between $\lambda/8$ and 2λ , where λ is the wavelength at the geometric mean frequency of the band over which the frequency is varied; 2) The bosses are sufficiently far apart for mutual effects to be neglected. This conclusion is tested for various numbers and configurations of bosses and over a range of bandwidths. Extension of this result to irregularly shaped, imperfectly conducting obstacles is also discussed.

¹ L. A. Lyons and A. T. Adams, "A Statistical Analysis of Siting Error in Radio Direction Finding," paper presented before URSI Fall Meeting, Palo Alto, Calif., December 1966.

1/6-2 PRECISION HIGH-GAIN ANTENNA MEASUREMENTS UTILIZING COMMUNICATIONS SATELLITES AND RADIO STARS. Stephen L. Zolnay and Curt A. Levis, ElectroScience Laboratory, (formerly Antenna Laboratory), Department of Electrical Engineering, The Ohio State University, 1320 Kinnear Road, Columbus, Ohio 43212

In this paper, techniques for the calibration of large antennas with very high precision are discussed. Communications satellites and radio stars were used as sources for measuring gain, and radiation patterns of a thirty-foot paraboloid at X-band. Freedom from ground reflection effects,

6

1

and the excellent agreement between the two independent measurements, allow high confidence in the results. The polarization pattern, and the noise temperature of the antenna were also precisely determined.

Since the flux from the communications satellites was not known accurately, a comparison method was used for determining antenna gain with this source. The antenna used for comparison was a 3-foot paraboloid whose characteristics were measured with extreme precision. The fluxes of several of the radio stars are quite accurately known making these stars very useful as sources in calibration experiments. This technique is also a comparison method, however, the standard used is, in effect, the antenna which was used to measure the flux of the star rather than a locally developed gain-standard antenna. The above two techniques of measurements are independent. To obtain quantitative information on the accuracy of the measurements, a carefully formulated error analysis of the data was carried out.

The gain measured by gain-comparison was 53.35 dB with random errors of ± 0.03 dB at the 99.7% confidence level and with additional uncertainties less than 0.39 dB in absolute magnitude. The corresponding results with Cassiopeia-A were 53.31 dB with random errors ± 0.09 dB with 99.7% confidence and with additional uncertainties less than 0.19 dB.

* The work reported in this paper was supported in part by Contract No. F30602-67-C-0119 between Air Force Systems Command, Research and Technology Division, Rome Air Development Center, Griffiss Air Force Base, New York and The Ohio State University Research Foundation.

1/6-3 OPERATIONAL COMPATIBILITY OF THE APOLLO HIGH GAIN ANTENNA. Donald S. Eggers, H. Dean Cubley, and Jefferson F. Lindsey, III, NASA-Manned Spacecraft Center, Instrumentation and Electronic Systems Division, Antenna Systems Section

6

Extensive tests have been performed at the Manned Spacecraft Center (MSC) to determine the effect of ground station modulation on the tracking capability of the Apollo command and service module high gain antenna. The tests were performed in the MSC radio frequency anechoic chamber with the Apollo high gain antenna, the Apollo S-band transponder and ground station equipment which simulates the Manned Space Flight Network. The high gain antenna consists of an array of four 31 inch diameter dishes and utilizes RF tracking with PIN diode switching. The PIN diode switching rates of 50 and 100 hertz provide the necessary phase shifts to generate the sum and difference patterns in both the azimuth and elevation planes. The effect of 20 different Apollo modulation parameters on the tracking performance of the high gain antenna in the automatic tracking mode was

investigated. This investigation revealed that the introduction of modulation on the up-link carrier caused a significant amount of degradation in the tracking capability of the high gain antenna. In particular, the test data indicates that the combination of voice on the 30 KHz subcarrier and the ranging code causes intermodulation products that degrade the tracking performance to the extent that adequate communications are jeopardized. Additional testing indicated that a reduction in the ground station modulation indices is required in order to limit the tracking degradation to less than the level that can be tolerated on the Apollo Lunar Mission.

1

1/6-4 A METHOD FOR TRACKING CLOSELY SPACED RADAR TARGETS. G. E. Pollon, General Dynamics, Pomona Division, Pomona, California

The tracking of two closely spaced radar targets is treated from an estimation point-of-view in which the target positions and signal waveforms are taken as unknown and are observed, with noise, at the outputs of an arbitrary set of antenna beams. The maximum likelihood processor is found and shown to involve the formation of directional nulls at the estimated target positions. The estimation accuracy, under good SNR conditions, of this processor is found. For an uncorrelated-target separation of one-third of a λ/D beamwidth the loss in angular estimation accuracy is as little as 8 db, and decreases at a rate of only 6 db per separation halving. The degradation is greater however in the coherent CW target case. In addition these results are independent of the target power ratio.

The primary emphasis is on putting these results into practice. A double interferometer-like system, which takes advantage of the properties of the maximum likelihood processor, has been devised. This system is analyzed and found to be within 5 db of the above limiting value. An X-band model of this system has been built and tested in an anechoic chamber. This particularly simple system detects the presence of two uncorrelated targets at a separation of one-third beamwidth when the weaker one is only 5.5 db to 8.5 db (depending upon the power ratio) stronger than required for detection when alone, and at a separation of one-tenth beamwidth when 16 db to 19 db stronger than required when alone. The experimental results are in agreement with the analysis and, in particular, a 30 db SNR target could be detected and tracked at a separation of less than one-tenth beamwidth from a target 40 db stronger, in the uncorrelated case.

1/6-5 RESONANCE REGION SCATTERERS STUDIES BY A PARALLEL RAIL-LINE RANGE AND COMPUTER SIMULATION. G. Burke, E. Miller, A. Neureuther and G. Pjerron, MB Associates, P.O. Box 196, San Ramon, California

6

1

Although elaborate ranges exist for the experimental study of radar scatterers in the resonance region, there is an apparent need for a rapid and inexpensive pre-screening process. MB Associates has developed a parallel rail range** especially suited to this purpose. The use of experimental data obtained from this range together with a proven computational technique had greatly reduced the overall time, effort and expense in studying a given kind of scatterer.

The rail range is based on simulating a plane wave by a TEM WAVE propagating between the rails, and while somewhat limited by fringing and mutual coupling effects between the objects and the rails, it has the advantage that the object intercepts a much larger fraction of the illuminating power than it would in a three dimensional range. It is as a result much easier and faster to tune out the background scattering in the rail range, and thus to make measurements over a range of specified frequencies.

Cross section measurements obtained from the rail range have served both to verify the validity of results obtained from it, and also to establish the accuracy of some thin-wire scatterer computer programs for calculating the cross-sections of single elements or arrays of complex geometry objects. A comparison of some experimental and computed cross-section results will be presented, and the relative merits of the theoretical and experimental approaches to the study of a given type of scatterer will be discussed.

** M.J. Gans, "The Transmission Line Scattering Range", Proc. IEEE, 53, 8, 1081 (Aug. 1965).

1/6-6 A SPECTRALLY CODED RADIOMETER. G.J.M. Aitken, and R. Mills, Electrical Engineering Department, Queen's University, Kingston, Ontario, Canada

6

This paper describes a novel method of coding the input signal of a radiometer. Rather than switching, as is done in the Dicke System (temporal coding), the spectrum of the incoming signals is shaped (spectral coding) so that by means of a simple signal processing procedure the output due to the spectral shaping and detection require nothing more complicated than delay lines and a simple correlator. The sensitivity of this radiometer can be shown to be the same as that of the Dicke Radiometer for the case of small signals. The effects of gain and front-end temperature variations are the same as in the conventional two-channel correlation radiometer. The advantages of this scheme are: (1) adjacent channel interference is removed because there is no switch, (2) the instrumentation is somewhat simpler because the switch, switching oscillator, synchronous detector and tuned amplifier are replaced by the system of delay lines, and (3) only one amplifier is used which is a simplification over two-channel correlation radiometer. A radiometer based on this principle of operation has been constructed.

MICROWAVE MEASUREMENTS

H. M. Aitschuler, Chairman

- 1.1-1 BULK CONDUCTIVITY OF SEMICONDUCTORS DETERMINED FROM TE_{01}^o -MODE REFLECTIVITY OF BOULE SURFACE. Keith S. Champlin, Gary H. Glover and John D. Holm, Electrical Engineering Department, University of Minnesota, Minneapolis, Minnesota 55455

This paper describes an "electrodeless" technique for measuring microwave conductivity and dielectric constant of a bulk semiconductor boule without the necessity of fabricating samples. All that is required is that the boule be sufficiently large and that it have one planar surface. The planar surface is butted up to a flange terminating a circular waveguide. The complex TE_{01}^o (circular E-field) mode reflection coefficient at the surface is then measured with a reflection-coefficient bridge. Because of the particular properties of this mode, no contact impedance occurs as does in the case of the TE_{10} -mode. Thus the measurements yield the true bulk properties of the material. To demonstrate the technique, 48GHz and 70GHz measurements of the conductivity and permittivity of a number of semiconductor boules at room temperature are presented and shown to agree favorably with results obtained by other means.

- 1.1-2 EFFECT OF SURFACE ROUGHNESS ON ACCURACY OF CALCULABLE COAXIAL IMPEDANCE STANDARDS. Albert E. Sanderson, Gordon McKay Laboratory, Harvard University, Cambridge, Massachusetts 02138

Calculable standards of impedance for coaxial measurements are usually sections of transmission line with accurately-known lengths, diameters and conductivities. However, the calculations are valid only for smooth conducting surfaces, and it has been assumed that a slightly rough surface behaves for all practical purposes like a smooth surface at the mean position of the rough one. This assumption is not justified.

Experimental measurements over a wide range of frequencies, surface finishes and conductivities indicate that even relatively small amounts of roughness can affect the surface impedance more than skin effect, for which extensive corrections have been published. Roughness can increase markedly both surface resistance and inductance, causes a surface inductance that does not approach zero in the high-frequency limit (as does the

skin-effect inductance), and can triple surface resistance at the frequency of maximum loss.

1

A perturbation theory correctly predicts the high-frequency surface impedance, the presence of a low-frequency surface inductance (in addition to that of skin effect), and the frequency of the transition between the two. For surfaces more than slightly rough, however, the magnitude of the low-frequency surface inductance is greater than predicted, and there is an anomalous peak in surface resistance at the transition frequency.

1.1-3 COMPARISON OF ELECTRICALLY-LONG LINES USING SWEEP-FREQUENCY REFLECTOMETRY. L. E. Sweeny, Jr., Radioscience Laboratory, Stanford Electronics Laboratories, Stanford, California 94305

Feedlines in phased arrays are usually matched in electrical length to extreme accuracy. For very large arrays this must be accomplished by sounding the cables from only their terminal ends since the element ends are so remote and widely spaced that they are unavailable for practical measurements.

An easily implemented, simple swept-frequency technique for matching lines has been developed which allows quick measurements in the frequency range of interest, and works well for lines whose round-trip attenuations are as high as 40 or 50 db, a case where most other techniques fail. Identical swept-frequency signals are transmitted down two lines whose remote ends are open-circuited. At the input of each line this provides both a transmitted signal and a reflected signal the frequencies of which differ by an amount related to the length of the line and the sweep rate. These difference frequencies are derived for the two lines with diode detectors, and their phases are compared with an oscilloscope by using the standard ellipse method. Identical-length lines give a straight line pattern; lines having different lengths give an elliptical pattern whose eccentricity indicates the magnitude of the difference.

When 4800 ft. lengths of 1/2 in. foam-dielectric coax were compared in the frequency range of 24 to 26 MHz, differences in length of less than 3 in. could be easily seen.

* This work was supported by the Advanced Research Projects Agency through the Office of Naval Research, Contract Nonr-225(54)

1.1-4 AN ATTENUATION AND PHASE SHIFT DIVIDER CIRCUIT, R. W. Beatty and G. H. Fentress. Radio Standards Lab., NBS, Boulder, Colorado

An attenuation and phase shift divider circuit is described. It consists of a main channel and a decoupled channel, the phases of which are adjusted to be initially either coincident or opposite. The ratio of the signal levels in the two channels is set by the coupling and/or by level set attenuators. After initial adjustment, known changes in attenuation or phase shift in the decoupled channel will produce smaller corresponding changes in the circuit output. The ratio of the corresponding changes can be accurately controlled and predicted.

The circuit is useful for accurately producing small changes of attenuation such as 0.0001 dB and small changes of phase shift such as 0.02 degrees when using commercially available components. Applications include a step attenuator having a continuously controllable step, and a vernier attenuator and phase shifter. The vernier feature is useful for fine control in nulling circuits and for accurately reading between calibrated dial markings on attenuators and phase shifters.

1.1-5 THE PRECISION MEASUREMENT OF THE ABSORPTION LOSS FOR LOW-LOSS TWO-PORTS. David F. Wait Radio Standards Lab. NBS, Boulder, Colorado

A method of measuring the absorption loss in a two-port is described. The method presented is intended for room temperature components with reflection coefficients of less than 0.5. Because the thermal radiation of a lossy two-port is directly proportional to its absorption loss, the absorption loss can be determined by measuring the thermal radiation from the element. The element to be measured is inserted between an available power radiometer and a liquid nitrogen or liquid helium-cooled noise source. The effective temperature of the noise source is then reduced in temperature by pumping on the vapor of the cryogen until the radiation to the radiometer returns to the level it had before the element was inserted. Alternately, the absorption loss may be measured relative to a precision attenuator. The precision of the method for relative measurements is $\pm 10\mu\text{B}$ ($\pm 10^{-4}$ dB) for losses up to 0.2 dB providing the temperature of the element under test is held within ± 0.2 K and the detection system can resolve 0.01 K. As an example of the application of the system, the absorption loss of several tuners as a function of their reflection coefficients will be presented.

1.1-6 SUPERHETERODYNE MEASUREMENT OF MICROWAVE ATTENUATION AT A 10 kHz INTERMEDIATE FREQUENCY. Richard F. Clark, Radio and Electrical Engineering Division, National Research Council, Ottawa 7, Canada

The excellent relative frequency stability of the output of two microwave oscillators phase-locked to a common reference signal permits the use of an audio intermediate frequency in the superheterodyne measurement of microwave attenuation. The phase-lock feature also permits the

1

measurement of microwave phase at the audio frequency. The choice of the audio instead of the more conventional 30 MHz intermediate frequency is made on the basis of the low cost and convenient operation, for similar accuracy, of an audio ratio transformer and audio phase shifter compared with a 30 MHz cut-off attenuator and 30 MHz phase shifter. The 10 kHz IF is a compromise frequency low enough to permit use of a good commercial ratio transformer and high enough to ensure reasonably low noise contribution from the local oscillator.

A measurement system of this type has been operated at frequencies ranging from 2.5 to 18 GHz. The basic 0.75 to 1.0 GHz reference signal for phase-lock is taken from a frequency synthesizer and fed into harmonic mixers associated with the signal source and local oscillator. The outputs of the harmonic mixers go to phase discriminators which control the microwave oscillator frequencies. A reference 10 kHz IF signal for use in phase measurement or synchronous detection in attenuation measurement is obtained by mixing the outputs of the phase discriminator oscillators.

The precision of attenuation measurement at a signal frequency of 10 GHz varies from ± 0.0002 dB for an attenuation step of 10 dB or less to ± 0.001 dB for a 50 dB step.

1.1-7 A NEW TECHNIQUE FOR MORE ACCURATELY ESTABLISHING A STANDARD OF FIELD STRENGTH. R. A. Lawton, HF Electrical Standards Section, Radio Standards Engineering Division, Institute for Basic Standards, Boulder, Colorado 80302

A new technique is presented for establishing a standard of field strength using a conducting sphere. An analysis is made to determine the current on the sphere as a function of the electric field strength of an incident plane wave, a method of measuring that current using electronic circuitry and an optical indicator within the sphere is described and an intercomparison is made with an independent field strength standard.

This technique is a significant improvement over previous techniques in that it permits the absolute determination of field strength with a maximum uncertainty of 1 percent or less at 30 MHz. This technique is applicable to a broad range of frequencies and field strengths.

1.1-8 A METHOD FOR PHOTOGRAPHING MICROWAVES WITH A POLAROID FILM. Keigo Iizuka, Gordon McKay Laboratory, Harvard University, Cambridge, Massachusetts 02138

It has been found that a standard Polaroid film can be used to map electromagnetic fields. The principle involved is the temperature depend-

ence of the developing speed of uniformly exposed film. The electric field produces a heating effect in the silver halide grains by inducing current in them. The resulting increase in temperature is proportional to the square of the intensity of the field. Thus, a thermal field is produced in the film which is a replica of the intensity distribution of the electromagnetic field. The localized heating in the grains leads to localized increases in the development of the film. On the film a visible pattern corresponding to the field intensity distribution appears.

The new method is not limited to electromagnetic fields, but may also be employed to record any temperature distribution of the object.

Microwave holograph has suffered from the basic difficulty that there is no convenient analog of the photographic plate at microwave frequencies. This film technique partially solves the problems and may open up the field of microwave holography.

* Dr. Iizuka is now in the Department of Electrical Engineering at the University of Toronto, Toronto, Canada.



COMMISSION 2

RADIO AND NON-IONIZED MEDIA

Dr. D.C. Hogg, Chairman

Session	Pages
<i>2-1 PROPAGATION TECHNOLOGY IN TROPOSPHERIC SCATTER AND SATELLITE COMMUNICATIONS</i> 1400 Tuesday, 10 September Room 309RB Chairman: Prof. M. Loewenthal Northeastern University Boston, Mass. 02115	15-20
<i>2/6 -1 ROUGHNESS AND OTHER EFFECTS RELATED TO THE SURFACE OF THE EARTH (Joint with Commission 6)</i> 0900 Wednesday, 11 September Room 356EC Chairman: Prof. R.K. Moore University of Kansas Lawrence, Kansas 66863.....	21-25
<i>2-2 LINE-OF-SIGHT PROPAGATION AT OPTICAL AND MILLIMETER WAVELENGTHS</i> 1400 Wednesday, 11 September Room 309RB Chairman: Dr. J.W. Strohbehn Dartmouth College Hanover, N.H. 03755	26-30
<i>Business Meeting Immediately Following the Session 1730 approx.</i>	31
<i>2-3 REFRACTIVITY AND ASSOCIATED PARAMETERS IN THE TROPOSPHERE</i> 0900 Thursday, 12 September Room 355EC Chairman: Dr. K.R. Hardy Weather Radar Field Station Air Force Cambridge Research Lab. Sudbury, Mass. 01776.....	32-34
<i>2-4 EFFECTS OF ABSORPTION BY TROPOSPHERIC CONSTITUENTS</i> 1400 Thursday, 12 September Room 355EC Chairman: Dr. P.M. Austin Massachusetts Institute of Technology Cambridge, Mass. 02139.....	35-38

Commission 2 Sessions 2-3 and 2-4 are being held in conjunction with the AMERICAN METEOROLOGICAL SOCIETY

2



PROPAGATION TECHNOLOGY IN TROPOSPHERIC SCATTER AND SATELLITE

COMMUNICATIONS

M. Loewenthal, Chairman

2.1-1 INDIRECT ATMOSPHERIC MEASUREMENTS UTILIZING RAKE TROPOSPHERIC SCATTER TECHNIQUES, PART I: THE RAKE TROPOSPHERIC SCATTER TECHNIQUE
B. B. Barrow, L. G. Abraham, W. M. Cowan, and R. M. Gallant,
Sylvania Electronic Systems, Waltham, Massachusetts

Unusually detailed multipath resolution of the tropospheric-scatter medium has been obtained by incorporating Rake instrumentation into tropospheric transhorizon microwave experiments. Radiofrequency carriers at approximately 900 MHz, each binary phase-shift keyed at 10 megbauds by a pseudo-random sequence of digits and subsequently filtered to a 10 MHz bandwidth, were transmitted during separate experiments in February, and November and December, 1965, over two paths -- a 480-km over-land path near the eastern coast of the United States and a 614-km over-water path in the Caribbean. At the receiver an identical binary stream was used in a series of 10 cross-correlators (Rake taps) where each stream was delayed 0.1 μ s with respect to the stream in the preceding tap. This provided a multipath resolution of 0.1 μ s which, depending upon the path length and altitude, corresponded to a separation of the common volume into ellipsoidal shells varying in thickness from about 200 to 550 m.

The principal goal of the experiments was to record the randomly varying in-phase and quadrature components of each tap output and thus investigate the fluctuations in signal phase, as well as in amplitude, caused by fading. The test procedures also permitted multipath structure and Doppler shifts to be directly observed. Scattering functions, which clearly illustrate the distribution of received signal energy as a function of multipath time delay and Doppler frequency shift, were calculated.

In contrast to a multipath time-delay spread that was ordinarily less than 1 μ s for the over-water path, spreads of over 3 μ s were common for the shorter, over-land path. Typical fading rates and Doppler spreads were also markedly different--several fades per second over land versus one fade per several seconds over water. Although some of the observed variations can be attributed to differences in antenna size (8.5 m diameter for over-land, 18 m diameter for over-water) and pointing angle, others apparently result from different typical refractive structure (meteorological conditions) within the atmospheric common volume of the respective radio links. Doppler shifts of as much as 15 Hz, which probably resulted from off-great-circle antenna alignment, were observed on the over-land but not the over-water path.

2.1-2 INDIRECT ATMOSPHERIC MEASUREMENTS UTILIZING RAKE TROPOSPHERIC SCATTER TECHNIQUES, PART II: RADIOMETEOROLOGICAL INTERPRETATION OF RAKE ATMOSPHERIC STRUCTURE OBSERVATIONS. W. P. Birkemeier and D. W. Thomson, University of Wisconsin, Madison, Wisconsin

2

Atmospheric structure has been remotely sensed using coherent detection of the Rake tropospheric-scatter sounding signal. Knowledge of the signal multipath time-delay and Doppler frequency shifts permitted spatial resolution of the atmospheric scatterers and/or scattering layers. In contrast to Doppler radar, whose backscatter signal enables one to study the velocity and identity of cm-scale precipitation particles or "angel-type" refractivity gradients, the forward-scatter geometry of Rake permits investigation of the motion and structure of 10^2 to 10^3 cm-scale atmospheric features.

The troposcatter signal appears to propagate via scattering and/or partial reflection from preferred altitude zones, or stratified layers, whose refractive characteristics and vertical distribution depend upon synoptic meteorological conditions within the radio common volume. Using a model based on the constant-phase geometry of the bistatic circuit, the combined antenna patterns and the reflectivity of the tropospheric medium, the component of the wind normal to the radio propagation path as a function of altitude is deduced from the nature of the Doppler spectrum as a function of multipath delay. The amplitude and "shape" of the Doppler spectrum at each multipath delay depends upon the turbulent refractive properties of each atmospheric layer which contributes signal at that delay. In some cases simulated scattering functions based on an isotropic $11/3$ power-law turbulence spectrum are in excellent agreement with observed scattering functions. Quasi-specular signal components, normally attributed to reflection from elevated layers, were modeled using highly anisotropic refractive index space correlation functions. Excellent agreement has been established for at least some experiments between rawinsonde and Rake-measured wind profiles and between radio signals and tropospheric temperature inversion layers and layers of relatively greater thermal stability. Radio signal differences between the over-land and over-water paths can be qualitatively explained in terms of prevailing weather conditions in the respective common volumes at the times of the experiments.

2.1-3 A SIMPLE STATISTICAL MODEL FOR TROPOSPHERIC SCATTER. I. H. Gerks, Collins Radio Company, Cedar Rapids, Iowa

Recently reported observations of the effects of crosspath wind on the phase recorded on a 230-km, 810 MHz path have suggested that an important cause of fading is the horizontal drift of a series of scattering centers. A sustained Doppler shift, either upward or downward, could be produced by an upwind or downwind displacement of the antenna beams.

In this analysis, the scattered power is assumed to originate at discrete centers arrayed linearly transverse to the path and spaced somewhat irregularly. This array is allowed to move across the path, and the contributions of all scatterers lying within the antenna beams are summed by a computer for a large number of positions. The resultant amplitude and phase can be plotted versus array displacement, which is proportional to time in accordance with the assumed wind velocity. This leads to fading records which bear a striking resemblance to experimental recordings.

Various arguments can be adduced to indicate that this simple model is not unreasonable under some atmospheric conditions. The important conclusion is that very encouraging results can be obtained with a fairly simple program, and that a way is indicated for investigating the effects of changing parameters of the model arbitrarily.

2.1-4 PHASE AND AMPLITUDE MEASUREMENTS OF TRANSHORIZON MICROWAVES: VERTICAL SPACE CORRELATIONS. D. C. Cox and A. T. Waterman, Jr., Stanford Electronics Laboratories, Stanford University, Stanford, California

A 3 GHz transmission over a 102-mile transhorizon path is received on twelve vertically-spaced antennas. After being recorded on magnetic tape, the data are analyzed in a variety of ways. The present paper discusses the correlation between the amplitude of the signal received on one antenna and that on another, for variously spaced pairs of antennas, and for various time lags between the two. The results are compared with other received-signal characteristics. For example, cases in which the correlation remains high out to appreciable antenna spacings are associated with antenna-array response-patterns* indicative of a greatly restricted region of scattering; while cases in which the correlation goes negative at some spacings are associated with response patterns indicative of a multiplicity of scattering sources.

*"Phase and Amplitude Measurements of Transhorizon Microwaves: Vertical Angular Response Patterns," by D. C. Cox and A. T. Waterman, Jr., paper presented at 1968 Spring URSI Meeting, 9 - 12 April, Washington, D.C.

This work was supported by the U. S. Army Signal Corps under Contract No. DAAB07-68-C-0149.

2.1-5 RADAR CLIMATOLOGY OF SEVERE STORMS. Frederick J. Altman, Communications and Systems, Inc., Falls Church, Virginia

Both M.I.T. and McGill University have shown that attenuation (and hence scattering) along elevated paths is determined chiefly by severe

storms. This reduces the amount of data of interest, but increases the difficulty of its characterization. The storm models which have been proposed are reviewed and some generalizations suggested. For example, although Byers and Braham indicate a positive correlation between thunderstorm cell height and diameter, it is shown that for the volume swept by a radar, height and low-level coverage are negatively correlated.

Severe storm occurrence is derived from both radar and surface data, presenting both detailed examples to clarify the concepts, and such statistical data as is available. The radar data is found to be too limited in total duration, and the surface data is too limited by the density of the observing network, but initial estimates confirm the rarity of the important storms at a given point except in a severe climate. Topographic effects of rugged terrain, the St. Lawrence valley, and ocean proximity are pointed out.

2.1-6 PHASE ANOMALIES OF SIGNALS SCATTERED OVER 100- to 180-KM PATHS.

S. N. Watkins, Advanced Development Engineer, Sylvania Electronic Systems, Western Division

In the October, 1967, URSI symposium, an experimental program was described in which the phase front of P- and L-band signals was being examined over 100- to 180-KM troposcatter paths by using phase interferometer techniques. The first portion of that program has been successfully completed, and the data have been processed.

Some of the more interesting phenomena observed during the course of this program, such as phase scintillation, phase rate of change, phase-amplitude changes, and phase stability vs. scattering volume, will be discussed along with a few of the more surprising effects measured, such as the effect of an aircraft flying through the scattering volume, the dependence of the measured angle-of-arrival fluctuations upon the electrical baseline of the receiving antenna, and techniques that enable a distinction to be made between mountain top and a true troposcatter reflection. Additionally, some comparisons of phase-change rates vs. signal-amplitude rates will be discussed. The processed data will also be examined in terms of angle-of-arrival effects so that the results of this program can be compared with the results of other similar troposcatter studies.

2.1-7 HIGH-PRECISION MEASUREMENTS OF THE PERFORMANCE CHARACTERISTICS OF IN-ORBIT IDCSP SATELLITES. Stephen L. Zolnay, ElectroScience Laboratory, (formerly Antenna Laboratory), Department of Electrical Engineering, The Ohio State University, 1320 Kinnear Road, Columbus Ohio 43212

For proper utilization and evaluation of communications satellites it is necessary to know their performance characteristics. The principal

parameters of the satellite which characterize its performance are the maximum effective radiated power (ERP), the power transfer, and the band-shape. Techniques, experiments, and their results are presented on the measurements of the parameters of the IDCSP satellites. These are hard-limiting (non-linear), wide-band communications satellites operating on X-band frequencies in nearly synchronous orbits. The experiments were carried out with a ground-station system which was calibrated to an unusual degree of accuracy (see accompanying paper: "Precision High-Gain Antenna Measurements Utilizing Communications Satellites and Radio Stars").

The maximum ERP was measured as a saturating cw signal was transmitted to the satellite. By measuring the variations in ERP as a function of input power and frequency the power transfer and the band-shape of the satellites were obtained. The polarization patterns of the received signals were measured and the apparent rotation of the tilt angle of these patterns caused by orbital changes was calculated. In this manner the polarization patterns were referred to the satellites and thus were made available to other observers. The amplitude scintillations in the signals were measured and the power spectral densities of these scintillations were computed. The ERP of the beacon channel and its variation as a function of coherent input power on the communication channel were also determined.

* The work reported in this paper was supported in part by Contract No. F30602-67-C-0119 between Rome Air Development Center and The Ohio State University Research Foundation.

2.1-8 TROPOSPHERIC SCATTER PROPAGATION AT 16 GHZ OVER A 500 KM PATH.

John W. B. Day and K. S. McCormick, Defense Research Telecommunications Establishment, Ottawa, Ontario and Uve H. W. Lammers and Edward E. Altschuler, Air Force Cambridge Research Laboratories, Bedford, Massachusetts

Results obtained from a troposcatter propagation experiment between Boston and Ottawa with two very high resolution antennas are presented. The AFCRL 29-Foot Millimeter Wave Antenna with a half-power beamwidth of approximately $.16^\circ$ is used to transmit 2 kilowatts of cw power. The DRTE 30-foot Antenna with about the same beamwidth uses a phase lock receiver having a minimum bandwidth of 125 Hz and a noise level of approximately -140 dbm. The main objective of this experiment is to investigate lower atmospheric structure through the use of a small common volume which is relatively well defined in both height and geographical location. Computer control on both antennas permits rapid, simultaneous, synchronous scanning of the common scattering volume. Various scan modes are used, including horizontal, vertical, constant height, constant scattering angle, and raster, to provide information on the scattering cross-section of the common volume as a function of spatial coordinates. Received signals up to at least 30 dB above the noise level are observed. Measurements are also conducted with the antennas at fixed angles.

In addition lower atmospheric structure is studied using the moon as a reflector. Signals at high elevation paths with a S/N ratio of about 30 dB are obtained.

2

*ROUGHNESS AND OTHER EFFECTS RELATED TO THE SURFACE OF
THE EARTH*

R.K. Moore, Chairman

- 2/6-1 A PREDICTION MODEL FOR MULTIPATH PROPAGATION OF PULSE SIGNALS AT VHF AND UHF IN IRREGULAR TERRAIN. Hermann F. Schmid, Stanford Electronics Laboratories, Stanford University, Stanford, California

A prediction model is presented that permits estimation of the probability of occurrence of distinct multipath propagation of pulse signals at VHF and UHF in irregular terrain. The model applies to terrain characterized by an irregular distribution of obstacles such as hills, buildings, trees, etc., so as to make it impractical to calculate the effect of multipath propagation by diffraction of bistatic-reflection theory.

Statistical data on wave propagation over irregular terrain form the basis for the empirical model developed. Generally, the model predicts that (1) for constant transmitter-to-receiver separation, the amplitudes of the received echoes decrease with increasing echo delay, and (2) for constant echo delay, the echo amplitudes become less attenuated, relative to the amplitude of the direct-path signal, as the transmitter-to-receiver distance increases. The results obtained from the model for rural, hilly terrain and for a built-up metropolitan area are compared to available measured data.

*The work reported herein was supported by the Department of the Army, U. S. Army Research Office, Durham, North Carolina, Contract DAHCO4-67-C-0032.

- 2/6-2 PROPAGATION OVER IRREGULAR TERRAIN AT FREQUENCIES ABOVE 200 MHz
A. P. Barsis and M. J. Miles, U. S. Department of Commerce, Institute of Telecommunication Sciences, Environmental Science Services Administration Research Laboratories, Boulder, Colorado 80302

During the past several years a theoretical and experimental study of radio wave propagation in irregular terrain was undertaken in the 230 - 9000 MHz frequency range with the objective of determining transmission loss variability as a function of location and terrain type, and of the effects of shielding by vegetation or other terrain clutter. This program was performed with support from U. S. Army agencies.

Results are available in the form of location variability and height gain as a function of path length and frequency. It was assumed that

time variability is small at most of the distance ranges considered (0.5 to 120 km) compared to the location variability due to terrain irregularities.

In general, path-to-path variability is very substantial even in relatively smooth, open terrain (eastern Colorado). At 230 MHz, transmission loss data are spread over a range of about 30 dB for 10 paths each 20 km long which converged on a common receiving location. The corresponding range for 9190 MHz was about 50 dB, and appeared to be independent of the receiving antenna height which varied from 1 to 13 m above ground.

The effect of shielding the transmitting antenna (7 m above ground) by rows or groves of trees produced a mean increase in transmission loss of approximately 10 dB for frequencies up to and including 1850 MHz. This shielding effect increased to a mean of 20 dB at 4595 MHz, and 30 dB at 9190 MHz. Values as high as 50 dB were observed on one specific path. For all these observations the receiving antenna remained in a clear, unobstructed location, consequently, the increase in transmission loss appears to be independent of receiving antenna height.

2

2/6-3 RADAR DETERMINATION OF THE SURFACE HEIGHT DISTRIBUTION OF A RANDOMLY ROUGH SURFACE. A. K. Fung, Center for Research, Inc., University of Kansas, Lawrence, Kansas

A method is described by which a poly - chromatic radar together with a phase measuring device may be used to measure the surface height distribution of a randomly rough surface. Except that the surface is assumed to be generated by a stationary random process and that it is smoothly undulating so that the Dirchhoff's method may be used to calculate the backscattered field, there is no additional assumption that needs be made.

This method is particularly suitable for studying surfaces that are spatially anisotropic or possess asymmetric surface height distributions.

Similar method applies to the determination of the more important two dimensional joint surface height distributions. However, the problem is too complicated unless we require the surface roughness to be isotropic. Also, a bistatic polychromatic radar with two receivers will be needed to facilitate measurements.

6

2/6-4 RADAR SPECTRUM COMPRESSION. H. S. Hayre and R. F. Broderick, Wave Propagation Laboratories, Department of Electrical Engineering, University of Houston, Houston, Texas 77004

Theories on spectrum compression have been based on the assumption of a relatively smooth surface which produced a doppler return from individual microscopic scatterers. Although these theories implied that

the spectrum compression systems would be insensitive to terrain bias and fluctuation errors, flight tests indicated these systems were sensitive to terrain effects. Application of the sampling theorem reveals that a spectrum compression ratio can be defined which shows that the bandwidth is reduced but the frequency shift due to the mean slope of the reflectivity curve or terrain bias error must be compensated. Observing that spectrum compression depends on the recombination of coherent signals, it is shown that the reflectivity variance terms or incoherent components from a rough surface must be attenuated sufficiently in order for spectrum compression systems to function satisfactorily. In particular the radar return spectrum may be non-gaussian for a random rough surface, and the validity of the spectrum compression theories using gaussian spectrum must be re-examined.

*This work is sponsored by NASA Manned Spacecraft Center, Houston, Texas, under Contract NAS 9-7828.

**Professor and Director, Wave Propagation Laboratories.

***NASA Manned Spacecraft Center, Houston, Texas.

2/6-5 SEA CLUTTER MEASUREMENTS ON FOUR FREQUENCIES. John C. Daley, Naval Research Laboratory, Washington, D. C. 20390

The initial processing and analysis of radar backscatter data, recorded off the coast of San Juan, Puerto Rico in July 1965, has been completed at NRL. This data constituted part of a study conducted in conjunction with the Applied Physics Laboratory of Johns Hopkins University to determine the scattering mechanism involved in the generation of sea clutter. Utilized in this experiment were the NRL WV-2 instrumented aircraft with its four-frequency, pulsed radar system and a surface vessel equipped and staffed by APL for the purpose of gathering sea surface data in the form of stereo-photographs and wave buoy measurements.

Radar returns were collected nearly simultaneously on four frequencies: 428 mcs, 1228 mcs, 4455 mcs and 8910 mcs, and both linear and cross polarizations. The data was processed to obtain the normalized radar cross section, σ_0 , of the sea surface as a function of various parameters. In particular, the behavior of the median value of the cross section, σ_0 , was investigated as a function of wind direction, incident angle, polarization, radar wavelength and gross surface conditions of wind velocity and wave height, and its variation determined. The effect of upwind-downwind-crosswind relations is shown to be greater on the short wavelengths and horizontal polarization. The polarization ratio is shown to decrease with increasing sea state and to be a function of wavelength. As surface roughness increases, it is seen that σ_0 becomes independent of wavelength for vertical polarization, but maintains an inverse wavelength dependence for horizontal polarization. The results

given provide estimates of σ as a function of the above parameters over an angular range of 4° to 90° (vertical incidence) and from very calm sea conditions to the moderately rough state approximately described by Beaufort 4.

2/6-6 SPECTRAL CHARACTERISTICS OF A RADAR SIGNAL SCATTERED FROM A LARGE, IRREGULARLY-SHAPED, ROTATING TARGET. Donald E. Barrick, Battelle Memorial Institute, Columbus Laboratories, Columbus, Ohio 43201

2
A large, rigid radar target which is continuously changing its aspect in time with respect to the line of sight will produce Doppler shifts in the backscattered signal if the target surface is rough or irregular. These Doppler shifts may be classified as an overall frequency translation due to motion along the line of sight, and spectral broadening due to the rotation of the effective scattering centers on the object. The former translation is readily accounted for, while the latter broadening is the subject of this paper. In this analysis, the surface of the target is treated as a random variable. Then the statistical characteristics of the scattered signal, and in particular the average radar cross section and average signal spectrum, are related to the target surface statistics. The target parameters which affect the scattered signal properties include the average radius of the body as measured from a convenient internal centroid, the rms surface deviation about this radius, the rms slope of the irregular surface, the apparent angular velocity of the rotating target observed from the radar, the angle between the axis of rotation and the line of sight, and the wavelength. The derivation is based on the physical optics integral and a Gaussian description of the target surface.

When the mean radius of the body surface is small with respect to the rms surface deviation, the results can represent the return from an aircraft or missile. In this case, the signal spectral broadening gives rise to a type of noise called "glint" or angle scintillation at the radar receiver, and an estimate of the spectrum of this noise is necessary to analyze the tracking loop of the system. When the rms surface deviation is small compared to the mean surface radius, the radar cross section and signal spectrum describe the radar scatter from a rotating planetary surface.

6
2/6-7 SIMULATION OF THE LITHOSPHERE BY DIFFUSION OF SALT INTO AGAR AGAR. Keigo Iizuka, Gordon McKay Laboratory, Harvard University, Cambridge, Massachusetts 02138

Theoretical studies to investigate the VLF propagation in the lithosphere are complex owing to the fact that a substantial change in conductivity takes place in a distance of a few wavelengths and

both so-called ray theory and wave theory fail. Hence, an investigation by means of a model which simulates the original configuration as closely as possible is of special significance.

A model scaling factor of 10^5 and a model frequency of 114 MHz were used. An aluminum plane is used to represent the upper, highly conducting crust; a water solution of 0.2 mol. NaCl represents the earth mantle. The simulated profile of the conducting layer was obtained by the diffusion of sodium chloride into the agar agar layer through a porous film at the bottom. The depth of 30 kilometers from the surface to the mantle was scaled down to 30 cms. The study of the propagation of the VLF wave in a distance of 100 kilometers was made by moving the probe along the slot in the aluminum plane for a meter. The vertical field distribution in such an inhomogeneous medium was measured by inserting the field probe inside the medium.

* Dr. Iizuka is now in the Department of Electrical Engineering at the University of Toronto, Toronto, Canada.

LINE-OF-SIGHT PROPAGATION AT OPTICAL AND MILLIMETER WAVELENGTHS

J.W. Strohbehn, Chairman

2.2-1 MICROWAVE PROPAGATION THROUGH A TURBULENT MEDIUM. Steven F. Clifford, Radiophysics Laboratory, Dartmouth College, Hanover, New Hampshire

This paper is concerned with the calculation of the statistical properties of an electromagnetic wave propagating through an electrically neutral atmosphere. It is assumed that the fluctuations of the wave parameters are caused by variations in the refractive index due to turbulence. The method of spectral expansions is used to calculate amplitude and phase spectra for a range of frequencies containing both the optical and microwave cases.

The results obtained reduce to the familiar Rytov result in the optical range. In the microwave region a second peak in the amplitude and phase spectra is found when the spatial wavelength of the index of refraction variation is equal to the wavelength of the incident radiation. The effects of this second peak on the correlation functions will be discussed.

2.2-2 MEASUREMENTS OF THE ATMOSPHERIC MICROSCALE USING A SHORT OPTICAL PROPAGATION PATH. D. A. Gray and A. T. Waterman, Jr., Stanford Electronics Laboratories, Stanford University

A short ($L = 10$ m), optical ($\lambda = 6328\text{\AA}$) propagation path is used to measure light amplitude fluctuations at spaced receiving points (fractions of an inch apart) and from them infer the magnitude of the smallest scale-size (the microscale l_0) of refractivity variations. When the microscale l_0 is on the order of a Fresnel zone $\sqrt{\lambda L}$, the covariance of the logarithmic amplitude $C_\rho(\rho)$, as derived by Tatarski for an infinite plane wave, depends on the magnitude of l_0 , and also, on the shape of the index-of-refraction spectrum in the region of viscous dissipation. With this in mind, computations of $C_\rho(\rho)$ for various models of the index-of-refraction spectrum, and for various values of l_0 , were performed under the condition $l_0 \sim \sqrt{\lambda L}$. $\lambda = 6328\text{\AA}$, and $L = 10$ m, and 30 m were used in the computations. Experimental measurements of $C_\rho(\rho)$ were made, and the results compared with the computed functions. The comparison indicates l_0 was small for all atmospheric conditions encountered, ranging from a few millimeters at midday to about one centimeter at night.

2.2-3 A MILLIMETER WAVE PROPAGATION AND COHERENCE EXPERIMENT. G. O. Young and W. H. Kummer, Aerospace Group, Hughes Aircraft Company, Culver City, California

An experiment to study millimeter wave tropospheric propagation, particularly the coherence properties of such radiation, is described. The experiment is being performed on an 18 mile millimeter wave link between Baldwin Hills and Malibu, California. Separate systems are set up to transmit at 28.5 GHz, 39 GHz, and 90 GHz. The experiment is still in progress, and is set up to measure both amplitude and phase of the return signal; the results for amplitude data are presently available. The experimental results include the analog data, mean value recordings (as a function of time), probability distributions of the received signal in amplitude (which are compared with theoretical distributions), autocorrelation functions and corresponding spectral densities for various carrier frequencies, and cross-correlation functions and cross-spectral densities in both space and frequency. The experiment is intended to measure the coherence and other statistical properties in space as well as time by employing two antennas which are movable with respect to each other in a vertical plane. The space-time coherence properties of the wavefront and the effect of the medium on these properties can then be discussed.

The ultimate purpose of the processing is statistical analysis in order to get a complete statistical description of the medium. In particular, the coherence function, which is a space-and-time averaged correlation function between different space-time points on the received wavefront is to be determined.* In addition to correlation and coherence computations, the following statistical analysis can be carried out as well: stationarity tests, tests for randomness, probability density computations and goodness of fit tests, moment analysis, and spectral analysis.

ACKNOWLEDGMENT

The research reported in this paper was sponsored by the Air Force Cambridge Research Laboratories, Office of Aerospace Research, under Contract F19628-68-C-0118.

*G.O. Young and A. Ksienski, Space-Time Transcorrelation Theory for Information-Carrying Signals, IEEE Transactions on Antennas and Propagation, Vol. AP-15, pp. 163-171, January 1967.

2.2-4 PROPAGATION TESTS AT 27-40 GHz IN THE GREATER WASHINGTON, D. C. AREA. H. Lake and J. F. Roche, Raytheon Company, Norwood, Massachusetts 02115

A test program has been carried out in the Greater Washington, D.C.

area to investigate the feasibility of wideband transmission at millimeter wavelengths. Measurements were made between July 1967 through February 1968 over an 8-km path and between March through May 1968 over a 32-km path.

An experimental determination of the parameters significant in the design and assessment of the operational capability of communication systems propagating in the 27-40 GHz frequency band were made. These areas of interest included:

- (1) Attenuation due to the transmission medium under clear weather conditions.
- (2) Path loss due to rainfall.
- (3) Fading and bandwidth of the medium.
- (4) Modulation capacity.
- (5) Diversity improvement.

A description of the program, summary of the radio and meteorological data and conclusions relevant to the transmissions over both paths are presented.

2.2-5 NEW RESULTS ON MICROWAVE LINE-OF-SIGHT PROPAGATION. W. T. Barnett, Bell Telephone Laboratories, Inc., Holmdel, New Jersey 07733

Continuous amplitude measurements have been made for 68 days at a rate of 5 samples per second per signal for seven 4 GHz and six 6 GHz signals on a typical radio relay path. Identical measurements were also made for one 4 GHz signal on a second path having a common reception point with the first path. Some results of an analysis centered on the fade depth distribution for fades exceeding 20 dB will be presented. These are:

- 1) The fade depth distribution below 20 dB is essentially the same for all the signals within a common carrier band. Further, the distribution has the Rayleigh slope.
- 2) The single channel fade distribution at 4 GHz differs from that at 6 GHz on the same hop and is different for the same 4 GHz frequency on adjacent hops with a common receiving point. These differences as well as the absolute values agree with a recent analysis of some British data which incorporates the effects of terrain.
- 3) The performance of one-for-one frequency diversity can be

specified for either the 4 or 6 GHz bands by the ratio of two quantities. The first is the percent frequency separation between diversity components. The second is the non-diversity fade depth distribution. This model is based on the frequency diversity data and is in agreement therewith.

2.2-6 McSIR -- AN INTERFEROMETER METHOD FOR MORE ACCURATE MESO-SCALE INTEGRATED RADIO REFRACTIVITY MEASUREMENT IN REAL-TIME. James J. Lamb, U. S. Army Electronic Proving Ground, and Arthur V. Carlson, Atmospheric Sciences Laboratory Research Area, Fort Huachuca, Arizona

An advanced requirement in surveillance and radio equipment test methodology is much more accurate, real-time quantitative measurement of spatially integrated atmospheric refractivity to correct radar refraction errors, as well as to provide concurrent propagation data for meteorological research purposes. Feasibility of meeting this requirement has been the objective of a study of dynamic atmospheric effects on line-of-sight microwave propagation during 1967-1968 by the U. S. Army Electronic Proving Ground, in cooperation with the U. S. Army Atmospheric Sciences Research Area, at Fort Huachuca, Arizona, using an experimental meso-scale radio refractometer concept named "McSIR," for Mesocavity Specular Integrating Refractometer.*

The McSIR configuration is an obtuse triangle having a 4-GHz crystal-controlled transmitter at the obtuse apex, directed at a passive plane reflector (speculum) 1.24 Km distant at the acute apex, and a dual phase-lock receiver combination with coherent channels located at the third apex 0.25 Km rearward of the transmitter.

The master receiver is phase-locked to the transmitter CW signal and supplies coherent crystal-controlled local oscillator and reference oscillator voltages through multipliers and buffers to the slave receiver. Thus slow drift in transmitter frequency is prevented from affecting the measurements and the unique independent variable is phase difference between transmitted and received waves. Since this difference is directly proportional to variation in phase velocity of the two-way CW reflected signal, the recorded phase difference is the direct measure of variation in radio refractive index of the atmosphere between transmitter and reflector sites.

The measured output phase variation is directly related to refractivity by the expression $\Delta\phi/N = 360/\lambda \times \Delta n \times 2L_p$, or 12 degrees per N unit for this configuration. Measurement precision to 0.5 N unit (6 degrees variation) or better is achieved. Diurnal variation ranging well over 360 degrees or 30 N units has been measured under clear weather conditions, and over 480 degrees or 40 N units during a disturbed period. Continuous McSIR and concurrent meteorological data for a number of 100-hour weekly periods have been recorded during the different seasons for a total of several thousand hours. Correlation coefficient of 0.98 is typical. Rigorous tests of system stability and data repeatability demonstrate

excellent reliability.

McSIR is giving Army research meteorologists new information on small-scale atmospheric processes and has potential as a remote probe over paths several miles long. Measurable incremental refractivity due to heavy precipitation has been observed during the summer monsoon season and is under investigation for rate of rainfall gauging. A technique for on-line automatic radar refraction error correction is being studied for application of McSIR methodology to improve radio and radar seeing.

* Implemented with the assistance of Smyth Research Associates, San Diego, California under contract No. DAAD04-67-C0049.

2

1730 Wednesday 11 September

ROOM 309RB

BUSINESS SESSION FOR COMMISSION 2

2

REFRACTIVITY AND ASSOCIATED PARAMETERS IN THE TROPOSPHERE

K.R. Hardy, Chairman

- 2.3-1 RADAR DETECTION OF CLEAR AIR ECHOES. Isadore Katz, The Applied Physics Laboratory, The Johns Hopkins University, Silver Spring, Maryland, and Dwight Randall, Naval Research Laboratory, Washington, D. C.

2
Powerful narrow-beam radars are capable of detecting echoes from the clear atmosphere. Aircraft equipped with meteorological instrumentation have been vectored into these regions to measure the structure responsible for these echoes. A strong correlation is found between regions of large variance in refractive index and clear-air-echo regions. This large variance occurs as a result of air of different moisture and temperature properties being locally mixed. The radars detect these regions in the process of mixing. This indicates that the meteorologist has a new and powerful tool with which to probe remotely certain types of turbulent regions.

- 2.3-2 RADAR, AIRCRAFT, AND METEOROLOGICAL INVESTIGATION OF CLEAR AIR TURBULENCE. K. M. Glover, R. J. Boucher, H. Ottersten and K. R. Hardy, Air Force Cambridge Research Laboratories, Sudbury, Massachusetts

Simultaneous studies of the lower 15 km of the atmosphere by multi-wavelength radar, jet aircraft, Jimspheres, and special radiosondes have been conducted at the JAFNA radar facility at Wallops Island, Virginia. Below an altitude of about 6 km, most of the clear-air turbulence (CAT) is detected with the Wallops radars; however, the intensity of the radar echoes is not an indication of the intensity of the CAT, and not all of the clear-air echoes are associated with turbulence of a scale affecting aircraft. Most radar layers correspond in height to regions of marked humidity stratification but with slight or no accompanying temperature inversions. Seldom is the reported CAT intensity greater than light at these altitudes.

Above about 6 km, radar detections of clear-air phenomena are less frequent but are generally associated with significant turbulence. Much of the CAT reported by the aircraft at these higher altitudes is not accompanied by radar echoes. This turbulence is usually associated with large scale wind shear and Richardson numbers less than 1.0. Indications are that radars of sufficient sensitivity can regularly detect clear-air turbulence at altitudes at least up to the tropopause; however, a radar parameter other than reflectivity must be used to differentiate between turbulent and non-turbulent phenomena.

2.3-3 RADAR AND AIRCRAFT DETECTION OF TURBULENCE IN THE STRATOSPHERE.

R. K. Crane, Lincoln Laboratory, Massachusetts Institute of Technology, Lexington, Massachusetts

Nearly simultaneous observations were made of thin turbulent layers in the stratosphere using the Millstone Hill L-band Radar and an Air Force high-altitude research aircraft. A series of five tests were conducted during May and June of 1968 to sound the region of the atmosphere between the tropopause and a 20 km height at ranges between 60 and 200 km from the Millstone Hill site. On each test thin turbulent layers were detected above the tropopause both by the radar and by the aircraft. The aircraft did not carry special sounding equipment and the intensity of turbulence was subjectively determined by the pilot. For the five tests, 23 layers were encountered characterized as very light, four as light, and one as moderate. For these tests the radar detected thin scattering layers at the height of the aircraft encounter and near the horizontal position of the aircraft for five of the very light encounters, three of the light encounters and for the moderate encounter. The radar also reported layers not detected by the aircraft but in these cases the aircraft did not sound through the layer height at the horizontal position of the radar report.

The results of these tests show that thin turbulent layers that affect both the aircraft and the radar were present on each of the five days. Layers reported as having light or moderate turbulence by the aircraft were also indicated by temperature inversions in the radiosonde soundings and were generally detectable by the radar. Sufficient data was not gathered to state whether the radar detected layers not detectable by the aircraft.

* Operated with support from the U.S. Air Force

2.3-4 RADIO SCATTER IN THE BUOYANCY SUBRANGE. R. Bolgiano, Jr., Center for Radio Physics and Space Research, Cornell University

The role that stable stratification in the atmosphere plays in determining the spectral structure of refractivity fluctuations (and thus of the wavelength dependence of scattered radio waves) has been debated for some years. The present study, based on simple energy considerations, concludes that, of the models proposed, the one most consistent with the notion of a buoyancy subrange predicts a spectral form proportional to k^{-1} (as opposed to $k^{-5/3}$ for the Obukhov-Kilmogorov theory). The wavelength dependence of radio and radar scatter that would be associated with such spectral structure is compared with that of other models and a brief explanation is offered of the physical process that may account for this structure.

2.3-5 MONOSTATIC AND BISTATIC SCATTERING FROM THIN TURBULENT LAYERS IN THE ATMOSPHERE. R. K. Crane, Lincoln Laboratory, Massachusetts Institute of Technology, Lexington, Massachusetts

2

Measurements were made of the scattering properties of thin turbulent layers at and above the tropopause. The Millstone Hill L-band radar was used to measure the backscatter cross section per-unit volume of these layers as a function of time and space. An X-band forward scatter link was set up between Wallops Island, Virginia and Westford, Massachusetts to observe scattering from these layers. Although the radar could not provide observations of the common volume of the forward scatter link, for days where no clouds were observed in the vicinity of the tropopause, the radar observations of layers near the tropopause showed horizontal uniformity of height and backscatter cross section, and the radiosonde data taken near the radar and near the common volume showed similar wind and temperature structure near the tropopause, the signal strength on the forward scatter link and its dependence on scattering angle behaved in accordance with the prediction of turbulent scattering theory using the radar data as an input.

The radar observations have shown that on each day measurements were made, layers were detected near and above the tropopause. Turbulent layers in the stratosphere have been detected at heights up to 22 km. These layers provide one of the mechanisms for weak, long-distance troposcatter propagation.

* Operated with support from the U. S. Air Force.

EFFECTS OF ABSORPTION BY TROPOSPHERIC CONSTITUENTS

P.M. Austin, Chairman

2.4-1 ATMOSPHERIC ATTENUATION STUDIES IN THE 200-300 GHz REGION. F. T. Ulabý and A. W. Straiton, Electrical Engineering Research Laboratory, The University of Texas at Austin

The purpose of this paper is to investigate the absorption characteristics of the Earth's atmosphere in the 200-300 GHz frequency region of the electromagnetic spectrum. Instrumentation problems associated with coherent radiometric detection dictated the use of a wide band Germanium bolometer detector. Upon helium-cooling the Germanium element to 4.2°K, the bolometer was observed to have a noise equivalent power of 10^{-9} watts for a 1 Hz bandwidth.

2

Using the sun as signal source, measurements were made of the solar radiation reaching the Earth's surface at two zenith angles through a set of wire mesh bandpass filters. The filter's transmission responses were determined by scaling from lower frequency measurements using a 109 GHz transmitter-receiver system. The total zenith atmospheric attenuation was then obtained as a function of frequency through the use of a spectral convolution technique developed in this paper. The results, especially in the window between the 183 GHz and 325 GHz water vapor lines, seem to agree favorably with the calculated values made according to the Van Vleck-Weisskopf equations modified by the Schulze-Tolbert line shape factor.

* This research work was supported by Air Force Contract AF 33 (615)-2274, Wright-Patterson Air Force Base, Ohio

2.4-2 THE VERTICAL DISTRIBUTION OF TEMPERATURE FROM SKY BRIGHTNESS MEASUREMENTS OVER THE 50 - 60 Ghz BAND OF OXYGEN. G. Miner, W. J. Welch, and S. Silver, Department of Electrical Engineering and Radioastronomy Laboratory and Space Sciences Laboratory, University of California, Berkeley

The determination of the vertical distribution of temperature in the earth's atmosphere from the emission and absorption characteristics of the atmosphere in the region of the O₂ microwave band, 50 - 60 Ghz, is a subject of considerable interest at the present time. In this paper, measurements of "sky" brightness at six frequencies in the band 50 - 60 Ghz are reported and the general problem of the absolute measurement of sky brightness in the zenith direction is treated. The required accuracy of the measurements is discussed in relation to calculations of the emission spectra made on the basis of a distribution profile obtained from radio-

sonde data obtained in close time relation with the radiometer measurements. This comparison provides a basis for analyzing the inversion problem -- the solution of the integral equation giving the brightness temperature as a function of frequency in terms of the distribution function and temperature profiles -- and the application of the Strand-Westwater theory for the inversion is discussed in the light of the present data and calculations.

* Work supported by the Air Force Cambridge Research Laboratories under Contract Number AF-19628-68-C-0022.

2.8-3 SOME MEASUREMENTS OF ATTENUATION BY STORMS USING A 16-30 GHz SUN TRACKER. D. C. Hogg, J. T. Ruscio, and R. W. Wilson, Bell Telephone Laboratories, Inc., Crawford Hill Laboratory, Holmdel, New Jersey

Data on storms observed during the first six months of 1968 are discussed. The ratio of the 30 to 16 GHz attenuation is found to be a function of the attenuation for most storms; this effect is related to the changes in drop-size distribution with rain rate. A comparison of attenuations obtained (at a given frequency) by measurement of the decrease in the signal from the sun (direct method) and by thermal emission from the rainstorm (radiometer method) is made. In this way the brightness temperature of the rain is estimated. Cases are discussed where this temperature is near 273°K; this low value is believed due in part to the significant scattering cross-section of the raindrops at these frequencies.

2.4-4 SIMULTANEOUS RADAR AND RADIOMETER MEASUREMENTS OF RAIN SHOWER STRUCTURE. R. K. Crane, Lincoln Laboratory, Massachusetts Institute of Technology, Lexington, Massachusetts

Simultaneous measurements of the backscatter cross section per-unit volume and the sky temperature were made for limited volumes of rain showers using an L-band radar and an X-band radiometer. The object of the measurements was to provide data to validate the method used to compute attenuation and sky temperature given weather radar data as an input and to investigate the special changes in rainfall intensity and in the attenuation cross section per-unit volume. The sky temperature was calculated using the radiative transfer equation and the distribution of attenuation cross section per-unit volume estimated from the weather radar data. An empirical relationship between attenuation and backscatter cross sections was used based upon the results of a large number of Mie theory computations using measured rain-drop size distributions.

The results of the comparisons between calculated and measured sky temperature show good agreement. The discrepancies between the measured and calculated values are due to the difference in the antenna beamwidths

for the two systems (0.5° for the L-band radar, 0.07° for the X-band radiometer). From these discrepancies the special distances over which the attenuation cross section can change significantly can be estimated. The results show that for the rain showers investigated the attenuation cross section per-unit volume can change an order of magnitude in 400 meters and the integrated attenuation along a horizontal line-of-sight can change an order of magnitude for 1.5 km horizontal translation of the path.

* Operated with support from the U.S. Air Force.

2.4-5 METEOROLOGICAL ASPECTS OF RAIN FALL ATTENUATION AT 11.7 GHz. Herman Lake, Raytheon Company, Norwood, Massachusetts

The results of a measurement and study program to investigate the reliability of transmission at 11.7 GHz and the relation of propagation effects and atmospheric parameters over an 11.42 mile path in Puerto Rico are presented. A comparison of observed and theoretical attenuation for various rainfall rates is given. A surface refractivity and refractivity gradient analysis indicates the temporal and spatial variations in the transmission medium.

2.4-6 REFLECTIVITY AND ATTENUATION MEASUREMENTS FOR TWO SUMMER SHOWERS. J. I. Strickland, Defence Research Board, Ottawa, Canada

Maps of reflectivity on a surface of constant elevation angle have been drawn for two summer showers using A-scan photographs obtained with an S-band radar. The photographs were taken at 10-sec intervals with the azimuth decreasing at approximately 8° min^{-1} .

The radar continuously tracks a CF-100 aircraft which flies in an arc centered on the radar and a 30-ft. precision tracking antenna located at the Defence Research Telecommunications Establishment, Ottawa, Canada. The signal strengths received by the tracking antenna from beacons at 4, 8, and 15 GHz carried by the aircraft are continuously recorded. The attenuation along a slant path is then known as a function of azimuth.

Integrated attenuations, calculated from the reflectivity using a relationship of the form $A = kz^\beta$, are compared with the measured attenuations at both 8 and 15 GHz. Since the interval between successive A-scan photographs is greater than that between successive attenuation measurements, the reflectivity maps are

used to deduce the reflectivity as a function of range at times coincident with the attenuation measurements. From these reflectivities, the variation of k and β with the structure of the storm is examined.

2.5-7 ATTENUATION STATISTICS FOR APPLICATION TO MICROWAVE COMMUNICATION LINKS. R. R. Rogers and K. M. Rao, McGill University, Montreal, Canada.

Radar records of thunderstorms in the Montreal area for a five-month period including the summer of 1963 were analyzed statistically to determine frequencies of occurrence of high attenuations over propagation paths in various directions. Results are presented for radio frequencies ranging between 5.5 and 45 GHz. For horizontal path lengths of 100 mi, it was found that the statistics for high attenuations (10 db and greater at 10 GHz) are essentially determined by rainfall rates of 25 mm hr^{-1} and greater, and are rather insensitive to the assumed form of the relationship between rainfall rate and attenuation.

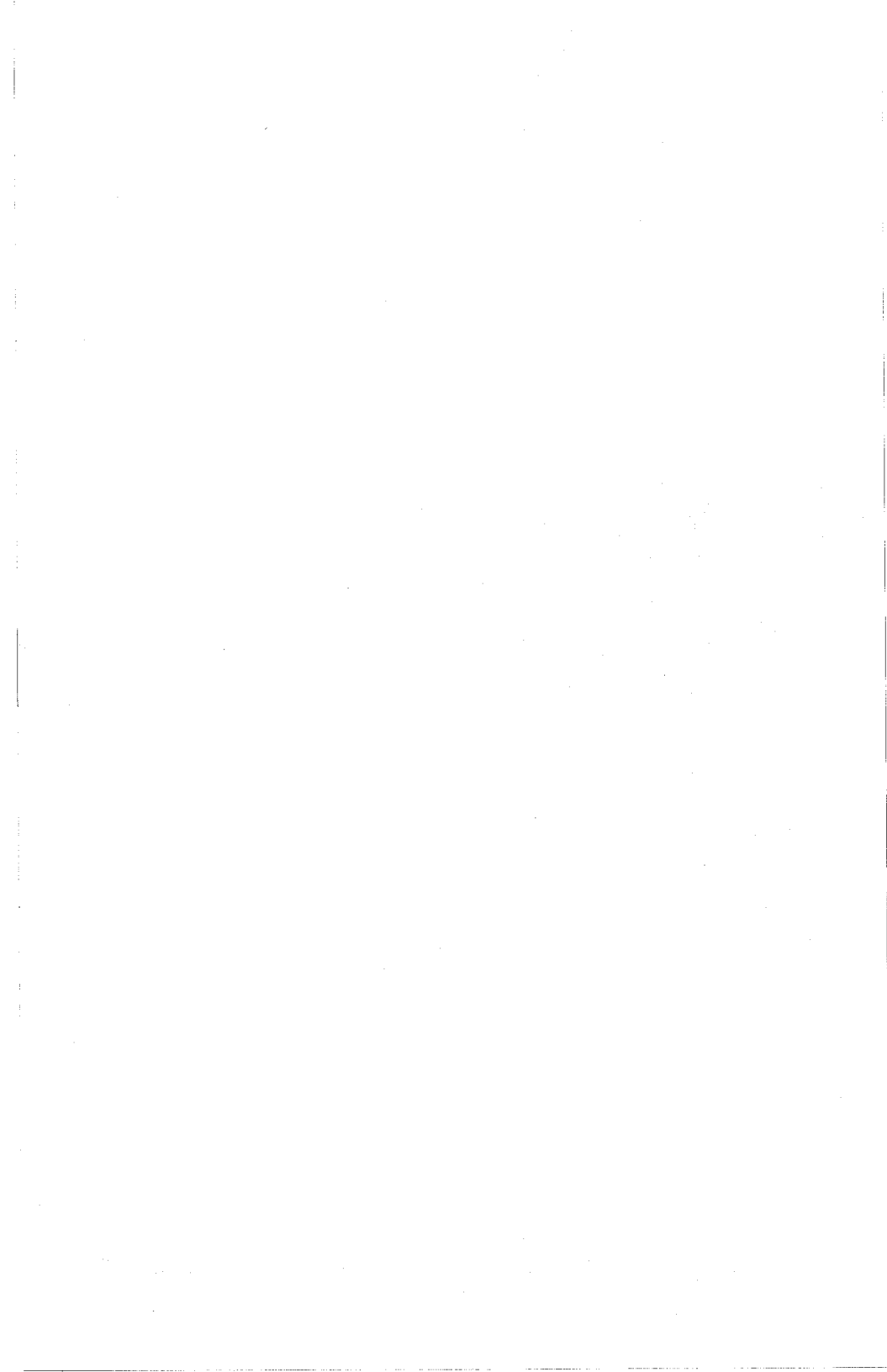
COMMISSION 3

ON THE IONOSPHERE

Prof. O.G.Villard, Chairman

Session	Pages
<p>3-1 <i>TRAVELLING DISTURBANCES</i> 1400 Tuesday, 10 September ROOM 307RB Chairman: Prof. R.D. Stuart Northeastern University Boston, Mass. 02115</p>	41-45
<p>3/4-1 <i>IONOSPHERIC THEORY</i> 0900 Wednesday, 11 September ROOM 307RB Chairman: Dr. J.V. Evans Lincoln Laboratory Lexington, Mass. 02173</p>	47-51
<p>3-2 <i>OBLIQUE PROPAGATION</i> 0900 Wednesday, 11 September ROOM 309RB Chairman: Prof. S.S.Sandler Northeastern University Boston, Mass. 02115</p>	52-55
<p>3-3 <i>SOLAR X-RAYS AND THE IONOSPHERE</i> 1400 Wednesday, 11 September ROOM 307RB Chairman: Prof. M.G. Morgan Dartmouth College Hanover, N.H. 03755</p>	56-60
<p><i>Business Meeting Immediately Following The Session</i> 1730 approx.</p>	61
<p>3-4 <i>TOPSIDE SOUNDINGS AND IONOSPHERIC STRUCTURE</i> 0900 Thursday, 12 September ROOM 356EC Chairman: Prof. M. Loewenthal Northeastern University Boston, Mass. 02115</p>	62-65
<p>3-5 <i>IMPROVED UTILIZATION: DRIFT AND RECOMBINATION</i> 1400 Thursday, 12 September ROOM 356EC Chairman: Prof. H.R. Raemer Northeastern University Boston, Mass 02115</p>	66-69





TRAVELLING DISTURBANCES

R.D.Stuart, Chairman

3.1-1 MID-DAY IONOSPHERIC SCINTILLATIONS AT MID-LATITUDE. R. S. Allen and J. Aarons, Air Force Cambridge Research Laboratories, Bedford, Massachusetts

The diurnal behavior of ionospheric scintillations has been studied at Hamilton, Mass., using two observational programs. In the first, the scintillation of the 54 MHz beacon of the satellite Transit 4A and of the 40 MHz beacon of the S-66 satellite, BE-B, have been examined in the region 35° to 50° N. Lat., 60° to 80° W. long. Results indicate the persistence of the usual nighttime maximum throughout the year. During magnetically quiet times; the K index of Fredericksburg, Va. equal to 0 and 1; therefore is a strong daytime maximum near local noon for the months of May, June, July, and August. As the state of magnetic activity increases, the daytime scintillations weaken and then disappear.

Unfortunately, for observations made either with radio stars or with low altitude satellites, the effects of seasonal change cannot be separated uniquely from the effects of diurnal change. The second program uses the synchronous satellites, Early Bird, Canary Bird, and ATS-3. The beacons (136/137 MHz) are observed continuously at nearly fixed geometry, therefore, seasonal and diurnal parameters can be studied separately. Results from 1965 and 1967, by coincidence confined to May, June, and July, confirm the noontime behavior observed with the low altitude satellites.

Concurrent studies of the same signals from equatorial stations did not show appreciable daytime scintillation.

Possible causes suggested for the daytime maximum of ionospheric irregularities at mid-latitudes include:

1. Sporadic E features.
2. Acoustic or gravity wave disturbances ducted southward from high latitudes.
3. An F region cloud of irregularities tending to be confined to mid-latitudes.

The second program using Canary Bird, ATS-1, and ATS-3 is now providing continuous data for several stations during 1968 in an attempt to isolate the pertinent factors, particularly the role of magnetic disturbance. The first results will be described.

3.1-2 OBSERVATIONS OF TRAVELLING IONOSPHERIC DISTURBANCES USING STATIONARY SATELLITES. T. J. Elkins and F. F. Slack, Air Force Cambridge Research Laboratories, Bedford, Massachusetts

Observations, at a sub-auroral zone site, of transmission from certain geo-stationary satellites, have revealed an unusual regular type of fading, apparently due to diffraction from moving ionospheric formations. The velocity of movement of these electron density irregularities was measured by means of a spaced receiver network, which in turn, allowed their height to be computed, in several instances, as well as certain other parameters of interest. The fading is deduced to result from electron density discontinuities, with linear gradients $\sim 700 \text{ cm}^{-3} \text{ m}^{-1}$, and located usually near the F region maximum, which travel in a generally equatorwards direction at $\sim 50 - 120 \text{ m/sec}$. Apparent periodicity in many fading events, and an association with ionosonde - measured disturbance, suggest that the diffraction takes place at facets of travelling wavelike formations in the ionosphere. Additional observational evidence is presented to support a hypothesis of ducted acoustic - gravity waves, probably excited by impulsive auroral - zone events, and having horizontal wave - lengths of $\sim 50 - 100 \text{ Km}$, with latitudinal extent, on occasion, exceeding 1500 Km .

3.1-3 ACOUSTIC WAVES IN THE IONOSPHERE. N. Narayana Rao, Ionosphere Radio Laboratory, Department of Electrical Engineering, University of Illinois, Urbana, Illinois. G. F. Lyon, Physics Department, University of Western Ontario, London, Ontario. John F. Klobuchar, Air Force Cambridge Research Laboratories, Bedford, Massachusetts

An unusual traveling ionospheric disturbance has been detected from Faraday rotation observations of 40- and 41-MHz signals from the radio beacon satellite BE-B, inclination 80° , observed simultaneously at Urbana, Illinois (40.1°N , 88.2°W), Danville, Illinois (40.1°N , 87.6°W), London, Ontario (43.0°N , 81.3°W) and Hamilton, Massachusetts (42.6°N , 70.8°W) three of which are widely spaced. The fluctuations in the total electron content deduced from these observations are interpreted as a superposition of long period and short period acoustic waves with the periods equal to about 3.5 minutes and 15 to 50 seconds respectively. The magnitudes obtained for horizontal velocities of propagation average about 4.5 km/sec at 350 km height and indicate wavefront tilts averaging about 10° from the horizontal if the waves are assumed to travel at the speed of sound at 200 km height. Possible sources of the disturbance are discussed.

3.1-4 INTERFEROMETER OBSERVATIONS AT 138MHz DURING THE ECLIPSE OF 12 NOVEMBER 1966. Albert D. Frost and Ronald R. Clark, Antenna Systems Laboratory, University of New Hampshire, Durham, New Hampshire

To examine the influence of solar eclipse conditions on the

scintillation in radio signals from extra-terrestrial sources due to irregularities in the ionosphere, observations were made at Ancon, Peru using an interferometer with a 220 wavelength baseline during the eclipse of 12 November 1966. This location was selected to provide a line of sight to the strong natural radio source Virgo A which would intersect the center line of the sun's shadow at an altitude of 100 km at totality. During the interval after first contact the signal from Virgo A was obscured by three periods of strong radio activity due to a source on the sun. While the effective length of the interferometer as seen from the sun was sufficient to resolve the total disc, a strong localized source would be visible. Analysis of the phase of the solar signals relative to those from Virgo A provides an estimate of the actual source position. While data on scintillation during the eclipse are incomplete the levels noted correspond to those observed during the previous ten days.

This work was supported by the Atmospheric Sciences Section, National Science Foundation with the cooperation of AFCL and the Instituto Geofisico del Peru.

3.1-5 INTERACTION OF ACOUSTIC GRAVITY WAVES WITH THE IONOSPHERIC F REGION. P. B. Rao and G. D. Thome, Raytheon Company, Spencer Laboratory, Burlington, Massachusetts 01803

A series of experiments were conducted in Puerto Rico during the summer of 1967 in which a 3 station network of the HF phase path sounders was operated in conjunction with the AIO Thomson scatter radar. The purpose of these experiments was to observe a few traveling ionospheric disturbances in enough detail so that meaningful comparisons with acoustic-gravity wave theory could be made. A preliminary look at the experimental results has been given elsewhere¹. In this paper a quantitative comparison is made between these observations and the predictions of acoustic gravity wave theory. The observed period and horizontal phase velocity is used to predict the velocity field of the disturbance in the neutral gas. It is assumed that in the height range of interest the electron gas moves with that component of the neutral gas velocity which lies along the magnetic field. The continuity equation for electrons is used to compute the resulting variations of electron density as a function of height and time. The effects of zero-order vertical electron density gradients, recombination, diffusion, and production are considered. To within the uncertainty of the measurements and of the model atmosphere, the computed and observed electron density perturbations are in agreement.

¹Thome, G. D., On the Structure of Traveling Ionospheric Disturbances: Results of a Combined HF-UHF Radar Experiment, Fall 1967, URSI meeting.

3.1-6 THE INTERACTION OF TRAVELING IONOSPHERIC DISTURBANCES WITH HF RADAR PATHS. G. D. Thome, Raytheon Company, Spencer Laboratory, Burlington, Massachusetts

HF radar has been and probably will continue to be the most widely used method for studying large scale traveling ionospheric disturbances. A serious problem with this technique is the uncertainty as to where along the HF ray path the traveling disturbance imposes its signature upon the probing radar signal. It is often assumed that the interaction takes place at the reflection height since the ray path is most sensitive to electron density variations at that level. Others contend that some traveling disturbances are restricted enough in altitude so that there may well be no substantial electron density variation at the reflection height and consequently the perturbations observed must be imposed at lower altitudes along the less sensitive portions of the ray path.

This question is investigated experimentally starting from observations of typical traveling disturbances made with HF and UHF radars at Arecibo. A two dimensional electron density distribution is derived for the disturbance using three spaced HF radars to measure horizontal speed and the UHF radar to measure vertical structure. Rays are traced through this distribution to synthesize the signatures observed at HF. By artificially eliminating the disturbance over various height intervals and again synthesizing the HF signature, the relative contribution made to the signature at various heights can be studied. Support is found for both points of view given above, depending upon the height of reflection and period of the disturbance.

3.1-7 IONOSPHERIC DOPPLER SOUNDINGS OF STATIC ROCKET FIRING PERTURBATIONS. David G. Detert, Avco Corporation, Space Systems Division, Lowell, Massachusetts 01851

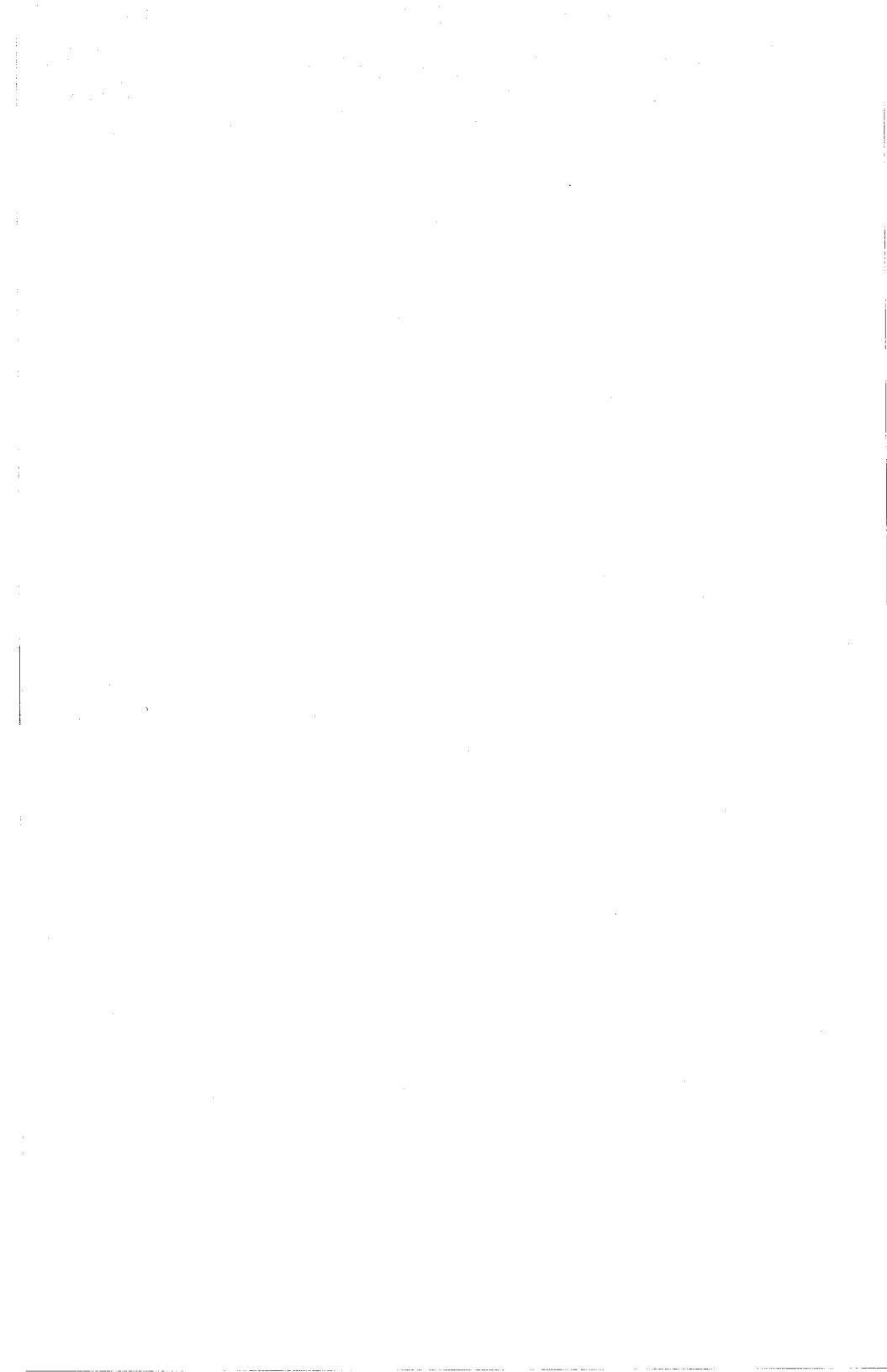
Preliminary results of fixed-frequency hf Doppler soundings taken on three simultaneous frequencies at Huntsville, Alabama, are presented. Three near vertical-incidence paths were operated simultaneously in a short-baseline triangular configuration.

Principal emphasis of the experiment was placed on detecting ionospheric perturbations following the static testing of large rocket engines at the NASA Marshall Space Flight Center. Effects related to the tests were observed on a limited number of occasions, with no apparent disturbances occurring during most of the firings. Relevant Doppler data are shown, and possible reasons for the apparent inconsistency of the results are discussed.

3.1-8 EARTHQUAKE EFFECTS OBSERVED BY OBLIQUELY PROPAGATED HF RADIO SIGNALS. D. E. Patton and C. Wilson, Raytheon Company, Burlington, Massachusetts

Data is introduced showing several ionospheric disturbances which followed the Alaskan Earthquake of 1964. A discussion of the

mechanisms believed to be the origins of these disturbances is given. The data consists of HF phase detected records of transmissions between Okinawa and Greece. Two distinct classes of disturbances are apparent on the records. The first, a spreading of the carrier frequency, is attributed to a coupled seismic-acoustic wave. Several seismic-acoustic modes are identified, and calculated arrival times are compared with the observed arrival time. The second class of disturbance, a coherent oscillation of the carrier, has four separate modes. The physical similarities of the four coherent modes suggest that all may be atmospheric waves with slightly different driving forces originating at the epicenter.



IONOSPHERIC THEORY

J.V. Evans, Chairman

3/4-1 TURBULENT PARAMETERS DETERMINED FROM RADIO METEOR TRAILS. S. P. Zimmerman, Air Force Cambridge Research Laboratories, L. G. Hanscom Field, Bedford, Massachusetts

The application of turbulence theory to atmospheric structure revealed by radio meteor trails clearly demonstrates that Batchelor's and Obukoff's structure function for isotropic turbulence explains some of the observed relations. From these measurements, parameters such as (the rate of viscous dissipation), u_k^2 (the eddy intensity of the scales up to k within the isotropic range), Re_k (the local eddy Reynolds number describing the turbulence up to a scale k), and χ_k (turbulent diffusion coefficient up to scale k), are determined. Also, an estimate of the rate at which turbulence extracts wind energy from the diurnal tide is given.

The results of the parametric study suggest very strongly that the universal range of the turbulent spectrum, in the upper atmosphere, contains little or no energy extending into the inertial subrange, but lies for the most part near the viscous (high wavenumber) region.

3/4-2 A THEORY OF E-REGION FIELD-ALIGNED IRREGULARITIES IN THE POLAR REGION. D. J. Fang, Radio Physics Laboratory, Stanford Research Institute, Menlo Park, California 94025

Following the suggestion¹ that in the lower E-region the horizontal wind-shear action may result plasma density irregularities, this paper examines the properties of the irregularities. It is found that the irregularities must be aligned along the magnetic field lines, and their transverse spatial scales remain essentially the same for all heights. The electric field which communicates along the magnetic field lines without much reduction of its strength is the main reason for keeping the irregularities aligned. The strength of the irregularity, defined as the density ratio of the irregularity to the ambient plasma, may increase significantly with height. For instance, for an irregularity of strength 1.2 at the height of 100 km, our theory indicates that the strength may reach 10 in the lower F region. This latter possibility may offer better explanations for certain radio anomalies, in particular the scintillations of radio star and spread F echoes².

1. D. J. Fang, "Horizontal Density Gradient of E-Region Irregularities Resulting from Atmospheric Turbulent Wind", URSI Spring Meeting,

April 9-12, 1968, Washington, D.C. Also, "Horizontal Wind-Shear Action and Its Resulting Irregularities in the Ionosphere", Symposium on Acoustic Gravity Waves, July 15-17, 1968, Boulder, Colorado.

2. Preferred URSI Commission: Commission 3, Ionospheric Radio.

3/4-3 THE DRIFT DISSIPATIVE PLASMA INSTABILITY AND EQUATORIAL SPREAD-F.

D. M. Connold, Harvard College Observatory, Cambridge, Massachusetts

3

Electrostatic oscillations of a plasma drifting across a magnetic field are considered. The convective instability which arises in a medium containing a gradient of electron density is investigated for the case when charged particle motions are dominated by collisions. The proposal that this instability is the amplification mechanism for producing the irregularities responsible for ionospheric spread F is examined. In particular the effect of the finite size of the irregularities in the magnetic field direction is examined. Qualitative consideration is given to the propagation of irregularities for realistic ionospheric electron density profiles. The velocity of the irregularities is equal to the electron drift velocity and an estimate is given of their amplification factor.

3/4-4 MULTIPATH EFFECTS IN TOPSIDE SOUNDING IN IONOSPHERIC DUCTS. Jerry Shmoys, NASA-Ames Research Center, Moffett Field, California

4

Ionograms which would be obtained by an ionosonde in a vertical depletion duct in a horizontally stratified isotropic plasma are calculated. In addition to the trace resulting from vertical (i.e., along the duct axis) propagation there are traces associated with ray paths making $1/2$, 1 , $3/2$, ... oscillations about the duct axis. It is shown that the shape of these traces depends very strongly on the manner in which the electron density varies across the duct. Ducts which are nearly homogeneous in the center and have large density gradients surrounding the central column yield "nose" shaped traces very much like those often seen on Alouette II ionograms. Electron density variation faster than quadratic with distance from duct axis is required for this type of trace. For ducts with slower than parabolic variation (e.g., Epstein type) the multipath traces split off from the non-oscillatory ducted trace.

Effects of relaxing the simplifying assumptions of this analysis (vertical duct direction, isotropy, cylindrical symmetry of the duct, etc.) will be discussed.

* National Research Council Research Associate on sabbatical leave from the Polytechnic Institute of Brooklyn.

3/4-5 IONOSPHERIC PHENOMENA BY COMPUTER EXPERIMENTS. James Fritz and K. C. Yeh, Ionosphere Radio Laboratory, Department of Electrical Engineering, University of Illinois, Urbana, Illinois

The unusual behavior in the F region ionosphere is known by a number of anomalies. Some of these anomalies have been with us for a long time. Many attempts have been made at explaining them and they have been hampered by the lack of exact information on the environment and on the precise rates of physical and chemical processes. This paper summarizes some preliminary results which aim to reproduce some of these unusual behaviors by computer experiments.

It is known that the electron density in the ionosphere at temperate latitudes satisfies a parabolic differential equation with certain boundary conditions. This equation can be solved numerically on a computer.

In this preliminary study we restrict ourselves to studying effects due to temperature dependent loss coefficient. Diurnal density profiles have been computed for different seasons and different solar epoch. Special computations have been made to study winter pre-dawn dip phenomenon which seems to be related to the time of sunrise at the geomagnetic conjugate point. The paper will be illustrated with a number of curves.

3/4-6 HYDROMAGNETIC WAVES IN THE IONOSPHERE AT LOWEST FREQUENCIES. H. Poverlein, Air Force Cambridge Research Laboratories, Bedford, Massachusetts

The hydromagnetic wave modes involving compression and expansion of the plasma - modified Alfvén waves and ion-acoustic waves - are considered in various frequency ranges extending to periods of approximately one day. The relationships between electric and magnetic fields, plasma flux and velocity, and plasma density oscillation in the individual modes are investigated.

The wave modes show quite different properties in different frequency ranges because of the varying role of the gravity force and of neutral-gas motion. At higher frequencies the ion-acoustic waves, which may be ascending or descending, entail significant variations of the plasma density. At lower frequencies two different ion-acoustic modes are obtained; both are evanescent, one is mainly connected with plasma motion, the other with density variations. At the lowest frequencies the modified Alfvén waves are the main carrier of plasma density variations. Coupling between the wave modes is decisive in all frequency ranges and may lead to simultaneous presence of all modes. Extrapolation to high and low altitudes indicates whether individual wave modes may originate above or underneath. Consequences of deviations from plane-wave theory at lower frequencies will be discussed.

3/4-7 VLF WAVE PROPAGATION ALONG A MIXED-PATH IN THE CURVED EARTH-IONOSPHERE WAVEGUIDE. David C. Chang, University of Colorado, Boulder, Colorado 80302

An investigation of very-low-frequency radio wave propagation across a land-sea boundary has been completed. Unlike most of the past investigations on this subject⁽¹⁾, the influence of the homogeneous ionosphere and the curvature of the earth, as well as the ground discontinuity have been considered. The problem of finding the field strength due to a horizontal line-source is first formulated as a Wiener-Hopf type problem, via the concept of equivalent surface impedance, and subsequently solved in the Fourier-transform plane. This solution has direct correspondence with that for dipole excitation, and is expressed analytically in terms of the reflection and transmission coefficients of modes in the two sections of the earth-ionosphere waveguide. Contrary to the theoretical results based on the ground wave propagation along⁽²⁾, the so-called recovery effect on both the amplitude and the phase of the receiving range. This confirms a prediction made in a previous paper by Wait⁽³⁾ who considered a similar problem, but with an entirely different approach. A numerical investigation of the effect of ground discontinuities for radio-wave propagation at 20 KHz was also made.

- (1) for example, D. R. Dobrott, "Propagation of VLF Waves Past a Coastline", Radio Science, Vol. 1, No. 12, December 1966.
- (2) J. R. Wait, "Electromagnetic Surface Waves", Advances in Radio Research, Vol. 1, 1964.
- (3) J. R. Wait, "Influence of an Inhomogeneous Ground on the Propagation of VLF Radio Waves in the Earth-Ionosphere Waveguide", Radio Science, Vol. 69D, July 1965.

3/4-8 ELF AND VLF FIELDS OF A HORIZONTAL ELECTRIC DIPOLE. Janis Galejs, Applied Research Laboratory, Sylvania Electronic Systems, Sylvania Electric Products, Inc., 40 Sylvan Road, Waltham, Massachusetts 02154

The waves in the spherical guide between the earth and ionosphere are excited by a horizontal electric dipole. The guide boundaries are characterized by surface impedances, and the resulting waves are expressed as a superposition of TM and TE modes. The wave numbers, excitation factors, height-gain functions, and height-dependent impedances are examined for both types of modes. For TM waves, the ionosphere appears in the VLF range as a nearly perfect reflector; but for TE waves, the same ionospheric model acts as a nearly perfect conductor. For TE modes, the excitation factor A_n is inversely proportional to the ground conductivity σ and is several orders of magnitude less than the excitation factor A_n^g of the TM modes. The height-gain function $G_n(z)$ is proportional to $\sqrt{\sigma}$ and is large in magnitude except at the ground surface where it is equal to 1 by definition; the TE modes are excited more efficiently by an elevated source.

A horizontal electric dipole is shown to provide a nearly omnidirectional coverage of horizontal field components in the frequency range of the lower Schumann resonances; and for an elevated source, the horizontal fields are essentially omnidirectional also in the VLF range.

The near fields of horizontal electric dipoles have been expressed as summations of wave-guide modes. Approximately 100 TM and 100 TE modes are necessary for representing the fields at a distance of 5 km from the source, but a smaller number of modes are sufficient at larger distances. In the vicinity of the source, the mode summations for the horizontal electric dipole compare with the relatively simple expressions for dipole fields on a flat finitely conducting ground plane. In the vicinity of the antipode, the vertical field components vanish; but the other field components remain of finite magnitude. This is opposite to the fields of a vertical electric dipole, where the horizontal field components vanish near the antipode.

This work was supported in part by the Office of Naval Research under Contract Nonr-3185(00).

3

4

OBLIQUE PROPAGATION

S.S.Sandler, Chairman

3.2-1 AMPLITUDE AND SPECTRAL CHARACTERISTICS OF HF RTW PROPAGATION. Charles A. Moo, AVCO Corporation, Space Systems Division, Lowell, Massachusetts 01851

The amplitude and spectral characteristics of pulsed and coherent around-the-world (RTW) transmissions, in the upper part of the HF band, from Manila at 320° azimuth are described. Measurements of amplitude were made by range sampling of the RTW delayed echoes during short pulsing periods every half hour. During the day, RTW signals of large amplitude propagate primarily when the transmitter-receiver pair are in daylight. The diurnal variation of signal amplitudes establishes the key role of sunrise and sunset tilts in RTW propagation, and supports a propagation model proposed by Isted (1958) in which rays originating from the ground are entrained through the night ionosphere in a ducted endoionic mode by these tilts, and makes possible propagation above the great-circle multihop MUF.

Besides the presence of the usual ionospheric disturbances, variations in the frequency spectra during coherent transmission periods exhibit unexpectedly large dynamic Doppler effects. On many days, wave-like undulations of the received frequency band by as much as 10 Hz about the transmitted frequency occurred for periods of hours. These disturbances appear when the southern propagation path is in night and seem to be most prevalent when the nearest approach to the southern auroral zone is at about 2200 geomagnetic time, corresponding to a time of maximum occurrence of precipitating electrons, as shown by Hartz and Brice (1967).

3.2-2 PRELIMINARY RESULTS OF A SATELLITE-TO-SATELLITE LONG-RANGE PROPAGATION EXPERIMENT CONDUCTED AT HF AND VHF IN THE LOWER IONOSPHERE. Mario D. Grossi, Raytheon Company, Sudbury, Massachusetts

A satellite-to-satellite propagation experiment at 21, 35 and 47 MHz was conducted between November 1966 and January 1967 to study long-range guided propagation, whispering gallery type, in the ionosphere below $F_2^{H_{max}}$.

Two satellites, a transmitting (OV4-1T) and a receiving (OV4-1R) one, were successfully launched in a 30° inclination circular orbit, 290 km high, and in two months of mission lifetime they became antipodal three times, due to a slight velocity differential imparted to them at injection into orbit.

Preliminary results of the data reduction and processing of the signals that OV4-1R received from OV4-1T indicate that low-loss receptions, implying guided propagation, took place at all frequencies up to antipodal distances. Path losses were often found smaller than either equivalent multihop or free-space propagation and were in agreement with the conclusions of a Hamiltonian ray-tracing analysis performed during the experiment design phase that predicted their value in the 125 to 135 db range.

The frequency of 34 MHz was the most effective and conditions of worst path losses were associated with 90° angular separation between the two satellites.

Multipath and doppler spreads were found less pronounced than for multihop propagation and smaller than expected from the ray tracing analysis. Pulses with 30 μ sec width have been received up to antipodal distances with well preserved shape. Wave coupling to the earth's surface for ranges beyond approximately 2000 km from the subsatellite point was weak and rare at 35 and 47 MHz.

We expect that these preliminary results of the OV4 experiment will be confirmed by the work underway. If these findings are then reproduced in future experiments, whispering gallery propagation paths will become attractive channels for long-range reliable communications between low-orbiting spacecraft.

*This work was supported by the Air Force Avionics Laboratory under Contract AF33(615)-1230.

3.2-3 COMPLEX ANGLES OF ARRIVAL. Samuel M. Sherman, RCA, Missile and Surface Radar Division, Moorestown, N. J.

The direction of arrival of a plane wave is conventionally defined as the direction of the normal to the phase front. However, when the arriving wave is the superposition of two or more (or a continuum of) plane waves of the same frequency but different directions, originating for example from unresolved radar targets or arriving simultaneously by different propagation paths, the conventional definition of angle of arrival is incomplete.

The definition can be generalized by making the angle of arrival a complex quantity. This is done by expressing it in terms of the gradient of the logarithm of the appropriate scalar component of the electromagnetic field. This gradient is in general the sum of two vectors with real and imaginary magnitudes respectively. The imaginary part is the phase gradient, the direction of which is the conventionally defined direction of arrival. The real part is the amplitude gradient, which in many cases is approximately normal to the phase gradient.

The component of the amplitude gradient parallel to the receiving antenna aperture can be measured by a simple addition to ordinary mono-

pulse techniques. This measurement is useful in analyzing the arriving wave and in matching the antenna weighting function to the wave to maximize received power.

3.2-4 ON EXTENDING THE AZIMUTHAL RESOLUTION OF HF RADAR ARRAYS, Bernard D. Steinberg and Mark S. Zimmerman, General Atronics Corporation, Philadelphia, Pa. 19118

A method is proposed for improving the azimuthal resolution of HF radar antenna arrays several times beyond the limitation due to ionospheric diffraction. Azimuthal resolution improves directly with array size, in accordance with standard array theory, until the beam width shrinks to a few degrees. Further increase in array size does not produce a dependable resolution improvement. In radio parlance, the signal is said to be decorrelated across the aperture. This "decorrelation" is due to diffraction by the nonhomogeneous ionosphere.

The diffracted energy accounts for only a portion of the received wave. The remainder, a near-specular component, not only has a very much narrower angular distribution of its energy, but appears to have a much longer (perhaps 100 times) time constant of fluctuation. This difference in fluctuation rate permits separation of the two components by filtering the received radar echo. The "decorrelating" component is thus reduced, as well as the diffraction limitation to the maximum useful antenna size.

A theory of resolution improvement through the use of filtering is described. When literature data are applied, it is shown that a several fold increase in azimuthal resolution is predicted. Introduction of additional data relevant to the theory will be encouraged from the floor.

3.2-5 LATERAL DEVIATION OF OBLIQUELY PROPAGATED HF RADIO RAYS. T. W. Washburn, Radioscience Laboratory, Stanford Electronics Laboratories, Stanford, California 94305

As is well known, magnetoionic splitting of obliquely propagated HF radio waves may result in deviation of such waves from the great-circle plane between transmitter and receiver. A computer ray-tracing routine has been employed at Stanford University to investigate the properties and maximum extent of this phenomenon under realistic ionospheric conditions. It is concluded that for a 1000 km path the difference in azimuthal bearing between the ordinary and extraordinary modes could reach a maximum of 0.5 deg, corresponding to an 0.25 deg variation of either mode from the true bearing. However, in most practical bearing estimation problems, the difference is an order of magnitude smaller than this maximum, and thus is truly small in comparison with other sources of error.

3.2-6 AN APPROACH TO MEASURING THE DIRECTION OF ARRIVAL OF RADIO WAVES IN THE PRESENCE OF WAVE INTERFERENCE. Jules A. Cummins and Stephen E. Cooper, Syracuse University Research Corporation, University Heights, Syracuse, New York

When two radio waves are reflected from the ionosphere and arrive at an antenna via two different elevation angles, the measurement of the angle of arrival of the stronger wave is influenced by the weaker interfering wave. Presented in this paper is an approach to measuring the elevation angle of the stronger wave.

Time variation is assumed in the field intensity of each wave and in their relative phase difference. The phase between two antenna voltages is measured, which yields an instantaneous elevation angle of the composite wavefront. It is then shown that the average phase corresponds to the phase associated with the stronger wave, provided the latter remains consistently stronger. An error with respect to this phase occurs if averaging includes values for which the weaker wave becomes momentarily stronger. A computer was programmed to generate the phase distributions for hypothetical situations. These distributions provide information as to the wide variations in the instantaneous phase calculations.

Experimental data were taken by a sampling process and averaging was performed to test the usefulness of the theoretical procedure. The results are correlated with the expected angles of arrival. The experimental and the computed phase distributions are compared:

3.2-7 HIGH RESOLUTION HF GROUND BACKSCATTER OBSERVATIONS. T. W. Washburn, Radioscience Laboratory, Stanford Electronics Laboratories, Stanford, California 94305

A bistatic HF backscatter sounder employing narrow, steerable antenna beams for transmitting and receiving has recently been placed in operation in the Central Valley of California. Antenna directivity at the receiver is achieved with a 2.5 km aperture; and an FM-CW exciter permits high time delay resolution and good interference rejection. Preliminary observations have revealed strongly enhanced echoes on group delay-frequency records which are thought to arise from relatively efficient scatter from ground features such as mountain ranges. These echoes are sharply defined in time delay and have a rather complicated structure. As many as ten different branches of such echoes are visible at times, which result from various combinations of upper, lower, ordinary, and extraordinary rays which are possible in two-way F propagation. Significant time fading and frequency fading is present on these echoes. Separate skip distance focusing lines in the backscatter are observed for ordinary and extraordinary propagation. Finally several manifestations of the effects of ionospheric disturbance phenomena are shown and discussed.

SOLAR X-RAYS AND THE IONOSPHERE

M.G. Morgan, Chairman

3.3-1 SOLAR X-RAY CONTROL OF THE E LAYER OF THE IONOSPHERE. P. R. Sengupta, Department of Physics and Astronomy, The University of Iowa, Iowa City, Iowa

Solar X-ray control of the E layer of the ionosphere is investigated. Electron density between 100 and 140 km above the earth on two typical days due to 20-100 Å solar X-ray flux is calculated using Explorer 30 (N.R.L. SR-8) data and is compared with observed electron density profile. foE/cos χ over Ottawa (45° N) and Washington (39° N) during November 1966 to March 1967 is seen to be closely related with 44-60 Å X-ray flux measured by N.R.L. detector on Explorer 30. Correlation with 8-20 Å flux is poorer. (foE)⁴/cos χ over Manila (15° N) and Breisack (48° N) during the period July 1966 to October 1967 exhibits a linear relation with X-ray flux. The relation is given approximately by:

$$(foE)^4 / \cos \chi = a + b \cdot F(20-100 \text{ \AA}) + c \cdot F(8-20 \text{ \AA})$$

where $a \approx 80 \text{ (mc/sec)}^4$; $b \approx 16 \text{ (mc/sec)}^4 \text{ per } 10^{-1} \text{ erg/cm}^2 \text{ sec}$; and $c \approx 1.8 \text{ (mc/sec)}^4 \text{ per } 10^{-2} \text{ erg/cm}^2 \text{ sec}$ when foE is expressed in mc/sec. These values are in good agreement with theoretical calculations. Constant "a" which gives a measure of ionization due to other radiations and hence is related to 11 year sunspot cycle, agrees well with the computed contribution due to EUV flux measured by satellite experiments.

Effective recombination coefficient of the layer calculated from the coefficients, a, b, and c, is in good agreement with accepted values.

3.3-2 SOLAR X-RAY CONTROL OF THE D-LAYER OF THE IONOSPHERE. P. R. Sengupta, Department of Physics and Astronomy, The University of Iowa, Iowa City, Iowa 52240

Solar X-ray control of the D-layer of the ionosphere is considered. X rays of wavelength less than 10 Å penetrate below 100 km without appreciable loss of energy at higher levels. It is, therefore, expected that 0-10 Å X rays would contribute to D-layer ionization. 2-12 Å X-ray flux data are available from University of Iowa detectors on Explorer 33 satellite. Flux below 10 Å is obtained from the available data assuming quiescent sun X-ray emission to be thermal in nature with $T_e = 2 \times 10^6 \text{ }^\circ\text{K}$. 0-10 Å is highly sensitive to solar activity level and varies within wide

limits over a period. It varied from a minimum of 2×10^{-4} to a maximum of 5×10^{-3} erg/cm² sec during the period July-December 1966.

Correlation between 2-12 Å⁰ flux and available daily and hourly D-layer indices are investigated. Daily variation of midday cosmic noise absorption at 30 mc/s over Bedford, Massachusetts, and daily variation of midday vertical incidence absorption at 2.4 mc/s over Breisach, Germany, are found to be well correlated with variations in 2-12 Å⁰ flux. 30 mc/s cosmic noise absorption over Bedford agrees with an empirical relation

$$A = .2 (\cos \chi)^{1/2} + 5.5 [F(2-12 \text{ Å}^0) \cos \chi]^{1/2},$$

where A is absorption in db, F(2-12Å⁰) is 2-12 Å⁰ flux in erg/cm² sec, and χ is the solar zenith angle. Computed value of absorption due to one erg of 2-12 Å⁰ flux agrees with the above relation. Theoretical computations and experimental observations have been combined to obtain the following relation for mid-latitude absorption

$$A/(\cos \chi)^{1/2} = \frac{180}{f^2} + \frac{500}{f^2} [F(2-12 \text{ Å}^0) \text{ erg/cm}^2 \text{ sec}]^{1/2}$$

where A is cosmic noise absorption in db at frequency f expressed in mc/s [f > 20 mc/s].

Electron production rates and electron density below 100 km are computed for the maximum and the minimum observed flux. It is shown that above 70 km ionization is determined chiefly by X rays. Below 70 km X-ray ionization is comparable with ionization due to Lyman alpha even for the observed minimum X-ray flux.

Lyman alpha flux is known to be fairly constant varying by a factor not more than 2 between solar minima and solar maxima. Thus the background (non-flare) 0-10 Å⁰ solar X-ray flux, which varies greatly with solar activity, is an important source of free electrons in the D-layer in two respects. First, the X-ray ionization over-rides the other sources of electrons down to 70 km during high or moderate solar activity. Second, even near minimum or low solar activity, daily or hourly variations in electron concentrations are caused by fluctuations in 0-10 Å⁰ flux.

The variation of D-layer height with solar activity cycle is also explained on the basis of relative importance of X-ray ionization over other sources of ionization.

3.3-3 ENHANCEMENT OF IONIZING RADIATION DURING A SOLAR FLARE. O. K. Garriott, Manned Spacecraft Center, Houston, Texas. A. V. daRosa and M. J. David, Stanford University, Stanford, California. L. S. Wagner, Arecibo Ionospheric Observatory, Arecibo, Puerto Rico, G. D. Thome, Raytheon Spencer Laboratory, Wayland, Mass.

Estimates were made of the enhancement in the ionizing radiation from the sun occurring during two important IIB flares which took place towards the end of May 1967. Increases in the solar euv radiation of about 10% were observed at the peak of the flares accompanied by a much larger (500%)₂ increase in the 45 Å X-ray band. The euv flux was augmented by $0.2 \text{ erg cm}^{-2} \text{ sec}^{-1}$ while the X-ray flux, below 160 Å, increased by about $0.9 \text{ erg cm}^{-2} \text{ sec}^{-1}$.

The above estimates were made using values of electron concentration in the lower ionosphere as observed by the Arecibo radar during the flares.

Values of the effective reaction rate α , and recombination coefficient β , during the preflare phase were computed from the observed electron concentrations and from calculated electron production rates. These production rates were determined by assuming a model atmosphere and a solar radiation spectrum and adopting the best available values for absorption and ionization cross-sections for the significant atmospheric gases.

3
Considering the time dependent continuity equation (but neglecting the diffusion term) and employing the observed values of n and dn/dt , flare enhanced values for the electron production rate were calculated using preflare values for α and β (depending on the altitude). Theoretical electron production rates were recomputed with a modified solar spectrum, the modifications in the fluxes being chosen so that theoretical and experimental production rates matched at all altitudes. In this manner it is possible to determine the time history of the solar flux at different wavelength bands during the flare. This work was supported by NASA grant NSG-30.

The present work has been supported by NASA grant NSG-30 and by the Arecibo Ionospheric Observatory operated by Cornell University with the support of the Advanced Research Projects Agency under a research contract with the Air Force Office of Scientific Research, OAE.

3.3-4 X-RAY EMISSION FROM THE QUIESCENT SUN--ROCKET AND SATELLITE OBSERVATIONS. P. R. Sengupta, Department of Physics and Astronomy, The University of Iowa, Iowa City, Iowa

Quiescent sun x-ray measurements made by different workers during the past nineteen years have been studied. Analysis of the data available upto April 1967 confirms that the quiescent sun x-ray emission is thermal in nature and is closely related to solar activity level. Spectrum below 18 Å is mainly continuous and is primarily due to recombination

emission, Bremsstrahlung becomes important at higher temperatures. 18-100 Å flux is primarily due to line emission and is emitted mainly by the undisturbed coronal regions. Below 20 Å, the emission is primarily from the active - hotter and denser - coronal regions. In this spectral region flux varies within wide limits, depending on number, dimensions, density and temperature of the active regions. Preferred regions of x-ray emission lie above strong calcium plages in the chromosphere and coincide with regions of enhanced centimeter radio emission. 75% of the total x-ray flux comes from these regions. The existing theory is capable of predicting x-ray flux within a factor of 2 or 3, using solar radio spectro heliograms in the centimeter range.

3.3-5 SOLAR X-RAY FLARES--ROCKET AND SATELLITE OBSERVATIONS. P. R. Sengupta, Department of Physics and Astronomy, The University of Iowa, Iowa City, Iowa

Rocket and satellite measurements of flare x-ray in different wavelength regions, including hard x-rays, are studied in detail. It is confirmed that in addition to enhancement of x-ray flux in all the wavelength regions, x-ray flares are characterized by hardening of the x-ray spectrum with appearance of hard x-ray in some cases. Probable flare x-ray spectral energy distribution is obtained from the spectral measurements made during past years. Correlation of x-ray flares with optical flares, radiobursts and S.I.S.s is considered in detail. Existing theories of x-ray flares are critically examined. Probable emission mechanisms are discussed and detail analysis is presented for two hard x-ray flares to show that hard x-ray flares may be due to non-thermal bremsstrahlung of non-relativistic electrons accelerated during the "flash" or the eruptive phase of the flare, while the accompanying centimeter radioburst may be due to synchrotron emission of the relativistic electrons. The soft x-ray component of the flare x-ray is found to be quasi-thermal in nature. It is concluded that x-ray flares are complex in nature and may belong to more than one class. Different competitive processes viz., appearance of new lines, quasi-thermal emission; non-thermal processes like non-thermal bremsstrahlung, inverse Compton effect and synchrotron radiation may simultaneously be responsible for flare emission in different wavelength regions. Of these bremsstrahlung, both quasi-thermal and non-thermal seems to be the most promising mechanism. New experiments are suggested for better understanding of solar x-ray flares.

3.3-6 THE DAY-NIGHT VARIATION IN POLAR-CAP ABSORPTION AND ELECTRON-LOSS PROCESSES IN THE LOWER IONOSPHERE. George C. Reid, Space Disturbances Laboratory, ESSA Research Laboratories, Boulder, Colorado 80302

During the major PCA event of September 1966, continuous measurements of 30-MHz absorption were carried out by a variety of riometers at high geomagnetic latitudes in both polar caps. The wide geographical coverage,

and the near-equinoctial timing of the event, led to essentially continuous coverage of both daytime and nighttime absorption throughout the event. The incoming proton spectrum was monitored at intervals of 1 - 2 hours by a proton spectrometer on board the polar-orbiting satellite 1963-38C (C.O. Bostrom, private communication), and the daytime and nighttime PCA were separately compared with the proton flux in the following four energy ranges: 1.2 - 2.2, 2.2 - 8.2, 8.2 - 25, and 25 - 100 Mev. The daytime absorption was found to correlate well with the flux in the two higher-energy fluxes. The implications of this result in terms of electron-loss processes in the lower ionosphere will be discussed.

3.3-7 IONOSPHERIC ABSORPTION AND THE ALBEDO EFFECT. Rosemarie A. Wagner and George J. Gassmann, Air Force Cambridge Research Laboratories, L. G. Hanscom Field, Bedford, Massachusetts

An aircraft carrying an ionospheric sounder traversed four times the boundaries of extended cloud cover near Los Angeles on 18 July 1967. Transmitting on 3 MHz the amplitudes of ionospheric E-layer echoes were received and recorded on magnetic tape. Median values of those amplitudes were determined in one minute intervals. Although these values scattered over ± 3 db, the average median was found to be lower by 3 db when the aircraft was over cloud cover, as compared to those intervals when the aircraft was over clear land. These results seem to suggest that an enhancement of the flux of visible light due to the reflecting cloud cover changes the chemistry of the D-layer in such a way that the electron density increases. An estimated 50% increase of the flux of visible light may thus be related to the observed 2 db increase of ionospheric absorption.

3.3-8 D-REGION STUDIES NEAR SUNRISE. A. J. Ferraro and H. S. Lee, Ionosphere Research Laboratory, The Pennsylvania State University

A high power wave interaction experiment is now in progress at the Ionosphere Research Laboratory for the purpose of measuring D-region electron densities and collision frequencies. Preliminary analysis of these results are presented and discussed for periods near sunrise. Such results will give a preliminary picture of the formation of D-region densities. Comparison with other workers is discussed.

*The research reported upon in this paper has been supported in part by the National Science Foundation under Grant GA-1456 and the Office of Naval Research under Grant Nonr 656(35).

1730 Wednesday, 11 September

ROOM 307RB

BUSINESS SESSION FOR COMMISSION 3

3

TOPSIDE SOUNDINGS AND IONOSPHERIC STRUCTURE

M. Loewenthal, Chairman

3.4-1 TOPSIDE IONOSPHERIC STRUCTURE AT NORTHERN LATITUDES AFTER GROUND SUNSET IN SUMMER. P. R. Arendt and H. Soicher, U. S. Army Electronics Command, Fort Monmouth, New Jersey

analysis of Alouette 1 ionograms taken shortly after ground sunset and during ionospheric sunset was performed for a magnetically quiet period in July 1966. The plot of electron density at fixed altitudes vs. latitude as the satellite moves northward (toward the midnight sun area) indicates that the density decreases at the lower altitudes (above h_{max}) and increases at the higher altitudes whereas there is no substantial changes in density at an altitude of 700 km. As the satellite enters the region of midnight sun from a region of darkness, a unique sunrise effect emerges. This effect is completely different from normal sunrise behavior.⁽¹⁾ During normal sunrise the red portion of the considerably-filtered solar spectrum heats the ionosphere causing thermal motions. The thermally-caused turbulence creates ionogram-spreading and amplitude scintillations of CW signals. In the region of the midnight sun, the ionosphere has already been illuminated for a long time so that the usually-observed thermal turbulence is not present. Our observations refer to the transition region between sunset and midnight sunrise. Here, the sounder explores the zone of twilight at various altitudes. Consequently no thermal turbulence can be expected and no spreading is observed on the ionograms.

(1) P. R. Arendt and H. Soicher, "Onset of Severe Amplitude Scintillations of Satellite Signals During Sunrise", Presented at '68 Spring URSI Meeting, Washington, D.C., April 10-12, 1968.

3.4-2 EFFECTS OF TWO MAGNETIC STORMS ON THE SOUTHERN HEMISPHERE TOPSIDE IONOSPHERE. Alan H. Katz, Avco Corporation, Space Systems Division, Lowell, Massachusetts 01851

Latitudinal profiles, from 10°N - 75°S , of plasma frequency at the height of the Alouette 1 satellite, and foF2 also observed by Alouette 1, are shown for two periods of time, each time interval containing a SC magnetic storm. In addition, electron density profiles from the satellite to the height of the F2 layer are compared for magnetically quiet and disturbed days during each time interval. The first magnetic storm occurred on 9 February 1963 with the SSC at 2102 UT, and the second occurred on 20 February 1964 with the SSC at 1137 UT. The available Alouette 1 data for this period of time occurred during midday for both magnetic storms.

The February 1963 storm was the largest of the two ($A_p = 45$ on 10 February 1963, whereas $A_p = 18$ on 20 February 1964) and correspondingly showed the largest effects. At high latitudes an increase in the plasma frequency at the satellite is observed on 10 February 1963. The increase in plasma frequency begins at $55^\circ S$, and at $70^\circ S$ (the furthest south for which observations are available) the plasma frequency is increased by 100% over the magnetically quiet days.

The first passes occurred 6 and 8 hours after the SSC of the 20 February 1964 magnetic storm. The pass at 6 hours shows no effects of the storm but the pass 8 hours after SSC shows a small increase of 0.2-0.3 MHz observed south of $50^\circ S$. An enhancement in the equatorial plasma frequency is observed, with a maximum increase of 30% between $10^\circ - 15^\circ S$ geographic, in the region of the magnetic equator. The percentage change decreases north and south of the latitude of maximum increase. The work was supported by the National Science Foundation under Contract NSF-C-515.

3.4-3 THE TOPSIDE EQUATORIAL ANOMALY. Charles M. Rush, AVCO Space Systems Division, Lowell, Massachusetts and Lawrence Lyons, Department of Meteorology, University of California, Los Angeles, California

Topside ionograms obtained by the Alouette I satellite over the equatorial region have been reduced to electron density profiles and analyzed for the period of October 1962 through April 1964. The equatorial anomaly is studied in detail as a function of local time and season for both the American and Japanese longitude sectors. It is found that the anomaly attains its maximum development around 1600 hours local mean time and persists somewhat through the night. It is better developed during the months surrounding the northern solstice and displays a marked longitude effect, namely, the anomaly generally extends to higher altitudes at the Japanese longitudes than it does in the American longitudes. Various transport terms that influence the development of the equatorial anomaly such as electrodynamic drifts and ambipolar diffusion are discussed in terms of the observed variations during both the quiet and disturbed magnetic conditions.

3.4-4 ANOMALOUS F-LAYER ENHANCEMENTS IN THE SOUTH ATLANTIC MAGNETIC ANOMALY G. J. Gassmann and C. P. Pike, Jr., Air Force Cambridge Research Laboratories, L. G. Hanscom Field, Bedford, Massachusetts

Ionospheric data show an anomalous F-layer enhancement during certain periods of the day in the area of the South Atlantic Magnetic Anomaly and its magnetic conjugate. Reexamination of IGY data confirms

the existence of these anomalies during most hours of the day and night in December with maximum activity occurring around 17 U.T. Electron density profiles obtained for several locations show details of the enhancement, and an attempt is made to relate them to electron precipitation from the Van Allen belts.

3.4-5 STUDY OF IONOSPHERIC ELECTRON CONTENT FROM OBSERVATIONS AT DIFFERENT STATIONS. M. Y. Youakim and N. Narayana Rao, Ionosphere Radio Laboratory, Department of Electrical Engineering, University of Illinois, Urbana, Illinois

Faraday rotation observations of 40- and 41-MHz signals from the satellite BE-B (inclination 80°) at Urbana, Illinois (40.069°N , 88.225°W) and Adak, Alaska (51.9°N , 176.5°W) during Jan.-Dec. 1966, at Bozeman, Montana (45.65°N , 111.05°W) during May-Nov. 1966 and at Houghton, Michigan (47.112°N , 88.689°W) during Apr.-Sept. 1966 have been used to obtain values of ionospheric electron content. The diurnal and seasonal variations of electron content and slab thickness and their latitudinal gradients are discussed. The midday values of electron content are combined with the values obtained by other workers at several stations including some from the southern hemisphere throughout the period 1958-1967 to study the solar cycle dependence of content. It is found that the 10.7 cm solar flux dependence of content exhibits an interesting hysteresis type of variation for both hemispheres but with different features. The well-known seasonal anomaly in midday content is also discussed.

3.4-6 ROCKET OBSERVATIONS OF ANTENNA IMPEDANCE AT VLF. R. E. Barrington, Radio Physics Laboratory, Defense Research Telecommunications Establishment, Ottawa, Ontario, Canada

A 200 foot dipole antenna was flown on a rocket launched near local midnight from Wallops Island, Virginia, in May, 1968. The antenna was excited at its mid point by a swept frequency source (0-15 kHz) and voltage and current magnitudes were measured at this point. From these measurements, information on the impedance of such an antenna at ionospheric heights from 100-800 km is presented.

A second 200 foot dipole antenna, orthogonal to the driven antenna and connected to a VLF receiver, observed the natural noise background, as well as the signals from the exciter. The amplitude and phase of the signals received from the driven antenna are discussed as well as the characteristics of the natural noise observed during the flight.

3.4-7 POLAR F-REGION TROUGHS. R. Penndorf, Space Systems Division, AVCO Corporation, Lowell, Massachusetts 01851

The presentation of foF2 data is accomplished best in form of synoptic and quasi-synoptic maps. A synoptic map shows the actual distribution of foF2 at a particular instance and it is given in U.T.; a quasi-synoptic map shows the monthly median foF2 at a particular Universal Time. We have constructed a large amount of such maps for the northern and southern hemisphere of which samples will be shown and discussed.

Comparing a large body of maps, we find that the strongest gradients of foF2 occur during the winter season; they are somewhat stronger in the southern hemisphere than in the northern hemisphere; but weak gradient persist throughout the summer season. The steepest gradients are found at sunrise. Troughs are found all through the year at all hours (U.T.) on the night side with its center towards the early morning. The main trough is aligned in east-west direction and moves around the Poles. The troughs are slightly deeper in the South Polar region than in the North Polar region. Subtroughs are seen in the northern hemisphere troughs.

The path of the troughs during a day is a very simple one during the equinoxes and winter; it follows more or less the geographic latitude of 60° with a disturbance whenever the trough approaches the Dip Pole meridian.

During the summer, however, the situation is different because the polar caps are continuously sunlit which leads to the existence of two troughs, one remaining mostly in the sunlit atmosphere, the "summer" trough, and another one in the night side, the "predawn" trough. The "summer" trough moves around the Antarctic Dip Pole in a closed loop with a radius of approximately 1500 km.

3.4-8 AIRBORNE OBSERVATION OF MIDDAY AURORA. J. Buchau and J. Whalen, Air Force Cambridge Research Laboratories, L. G. Hanscom Field, Bedford, Massachusetts and S. I. Akasofu, Geophysical Institute, University of Alaska, College of Alaska

On December 13, 1967, a KC-135 aircraft equipped with an ionospheric sounder, a photometer, and an all-sky camera made a flight into the midday portion of the auroral oval and polar cap regions between Greenland and Spitzbergen. During the quiet magnetic conditions ($K_p = 1$) prevailing on that day, the midday aurora was observed within the expected region of the oval and found to be absent within the polar cap region. The evaluation of the sounder data shows strong correlation between auroral E_s and visible overhead aurora. Near the end of the flight when sunrise prevented optical observations of the aurora, the observed occurrence of E_s agreed with the predicted region of the oval.

3

IMPROVED UTILIZATION; DRIFT AND RECOMBINATION

H.R. Raemer, Chairman

3.5-1 ADAPTIVE SIGNAL PROCESSING FOR IONOSPHERIC DISTORTION CORRECTION.
D. J. Belknap, R. D. Haggarty, B. D. Perry, The Mitre Corporation,
Bedford, Massachusetts

This paper presents a description of the on-going Mitre adaptive signal processing technique program which has as its goal the real-time correction of ionospheric distortion of wideband HF signals.

The practical feasibility of the correction technique has been demonstrated by experiment. The results of a computer study based upon data taken with the cooperation of Stanford University in February and June 1967 verify the non-real time capability of the technique. The correction of a vertical one-hop path at Mitre in Bedford, Massachusetts has demonstrated real-time capability.

The basic approach is to partition the problem into two parts: (1) a measurement problem wherein the ionospheric distortion characteristic is determined, (2) an adaptive processing problem wherein a receiver processor takes on an appropriate corrective characteristic for subsequent wideband transmissions. The processor is adaptive only in the sense that it is flexible and can be commanded to assume the proper characteristic (i.e., the output of the adaptive processor is not employed in a closed loop manner).

The method models the ionosphere as a linear system having a non-time varying transfer response. Consequently, all of the above operations must be accomplished before a significant change of the ionosphere takes place. Experiments performed to date reveal that correction dispersion can be accomplished and, once made, will not deteriorate significantly for many seconds (up to eighteen seconds in the case of the 900 kHz bandwidth on an oblique link). The more rapidly varying distortions, due to close and weak multipath, can also be compensated but for shorter periods of time.

Since the goal is to demonstrate the feasibility of ionospheric distortion correction, equipment employed to date has been simplified by using a linear FM signal, both for distortion measurement and for the subsequent transmissions to be corrected. Correction has also been restricted to a one-hop one-way transmission which is basic to all more complicated applications. The general applicability of the correction technique is not diminished by such economies.

With feasibility demonstrated, attention is now being directed toward questions related to the useful degree of path reciprocity as well as inverse filter realizations.

3.5-2 STORED IONOSPHERE - DEVELOPMENT AND USE. Bernard Goldberg, Communications/ADP Laboratory, U. S. Army Electronics Command, Fort Monmouth, New Jersey 07703

The Stored Ionosphere represents a new departure in multipath transmission simulation. By means of employing RAKE principles, it has been possible to record actual ionospheric path transfer functions on a continuous sampled basis. These recordings are then employed as function generators for an inverse RAKE which is utilized as the Multipath Transmission Simulator. An explanation of the basic principle of RAKE coupled with a discussion of how the channel measurement filters provide the appropriate analog of the ionospheric medium is undertaken. The necessary signal processing for the recording, playback, and operation of both the RAKE and the Stored Ionosphere Multipath Simulator, is covered in detail.

The basic difference between the Stored Ionosphere and other multipath transmission simulators lies in the fact that, in the Stored Ionosphere, the actual time variant dispersive properties of the medium are used as control functions, while in the other concepts, estimates on a gross basis are generally employed.

The utility of the device, in conjunction with a recorded library of tapes of the perturbed ionosphere, together with a description of its ease of deployment, and its potential as a test standard, are discussed in reasonable detail.

3.5-3 THE POTENTIAL EFFECTIVENESS OF A POLARIZATION DIVERSITY SYSTEM.

Joseph T. deBettencourt, James F. Roche, Carson K. H. Tsao, John S. Underwood, Raytheon Company, Norwood, Massachusetts 02062

A measurement program was carried out with the use of a Tapered Aperture Horn Antenna to investigate the potential of polarization diversity on long-haul HF circuits. Transmissions from Hawaii and San Francisco were received at the STRATCOM Washington Site at LaPlata, Maryland. Signals were received under a variety of diurnal, ionospheric and multipath conditions on horizontally and vertically polarized elements of the Tapered Aperture Horn Antenna. The data was analyzed and the degree of correlation between the orthogonally polarized signals was determined.

Measurements were also made of the effectiveness of polarization diversity using a HF Predetection Combiner. A comparison was made of the polarization diversity performances with space diversity system generally used. Both systems performed equally well under similar conditions.

The results of these sets of measurements indicate that HF polarization diversity can provide equal performance with space diversity systems while at the same time realizing savings in required antenna space and equipment complexity.

This work was conducted under Control No. DAAB07-67-C-0398 with the U. S. Army Electronics Command and also was sponsored in part by Raytheon Company under its Independent Research projects.

3.5-4 ELECTRON DRIFT IN THE IONOSPHERE NEAR THE DIP EQUATOR. V. L. Peterson and J. P. McClure, Jicamarca Radar Observatory, Apartado 3747, Lima, Peru

Electric fields generated in the ionospheric E region are responsible for the motion of the F-region plasma perpendicular to the earth's magnetic field. The velocity of this "drift" has been measured at the Jicamarca Radar Observatory by Doppler techniques; the spatial and temporal variations of this drift was the subject of an earlier URSI presentation. The present paper deals with the analysis of this data, together with simultaneous electron density and temperature data, by way of the equations of continuity and force for the electrons and ions. Because Jicamarca is near the dip equator the drift velocity is vertical, which simplifies analysis. In particular, the divergence of the horizontal component (along the magnetic field) of electron flux can be explicitly solved for. This term is found to vary greatly with time and altitude and at certain times and heights is larger than the corresponding vertical component. Below about 250 km, at least for this data (January 1968), electron motion (vertical plus horizontal) played no significant role in determining the electron distribution. Above this height, however, electron motion became increasingly more important, and by 400 - 500 km (depending upon the time of day) was dominant in determining the electron distribution. The implications of these motions on the latitudinal electron distribution and on the departures from the equilibrium distribution of ions will be discussed.

3.5-5 6300 A NIGHTGLOW AND ELECTROMAGNETIC DRIFT IN THE TROPICAL F² LAYER. T. E. VanZandt and V. L. Peterson, Jicamarca Radar Observatory, Apartado 3747, Lima, Peru

It is known that the variations of the 6300 A nightglow in the tropics are caused by variations in the rate of recombination in the F2 layer, due to changes in the electron density distribution is controlled partly by electromagnetic drift and subsequent diffusion along the magnetic field lines. These relations have been confirmed by observations of nightglow, drift, and electron density profiles at Jicamarca. It is shown that drift and diffusion probably also cause the variations of nightglow observed in the higher tropics, for example, from Hawaii. However, when the nightglow varies rapidly in both time and space, as it often does, the roles of drift and diffusion are quite different than they are during the steady-state conditions of the daytime equatorial anomaly. In particular, an enhancement of the nightglow is caused by a westward electric field, while the equatorial anomaly is caused by an eastward electric field. The reasons for this and the implications of the nightglow observations on the structure of the tropical F2 layer will be discussed.

* A cooperative project of the Aeronomy Laboratory, Environmental Science Services Administration, Boulder, Colorado, and the Instituto Geofisico del Peru, Lima, Peru.

3.5-6 RECOMBINATION IN THE F REGION OF THE IONOSPHERE FROM INCOHERENT SCATTER MEASUREMENTS AT ARECIBO. R. Warner and J. S. Nisbet, Ionosphere Research Laboratory, The Pennsylvania State University

A study has been made of the detailed behavior of the F region at night using the incoherent scatter sounder at the Arecibo Ionospheric Observatory to determine to what extent it is compatible with current laboratory reaction rates.

It was found that if currently accepted values for the ratios of the atom ion interchange reactions between atomic oxygen and molecular nitrogen and molecular oxygen are employed with the CIRA 1965 model atmosphere, then a production source of the order of 10^9 electrons $\text{cm}^{-2} \text{sec}^{-1}$ would be required. It is concluded that such ratios are difficult to reconcile with available production mechanisms.

The behavior if either the neutral molecular densities or the reaction rates are lowered by a factor of 3 is examined and it is shown that there is considerable detailed agreement between the calculated loss rates and the observed recombination rates. Additional production sources of the order of 10^8 $\text{cm}^{-2} \text{sec}^{-1}$ are then required after sunset and before dawn.

Photoelectron fluxes, horizontal ion velocities combined with horizontal density gradients and horizontal velocity gradients are examined as possible production sources.

This work was supported by NASA Grant Nsg 134-61. The Arecibo Ionospheric Observatory is operated by Cornell University with the support of the Advanced Research Projects Agency under a research contract with the Air Force Office of Scientific Research.

3

1944-1945
The following information was obtained from the records of the
Department of the Interior, Bureau of Land Management, at
Washington, D. C., on the subject of the above-mentioned

land. It is noted that the land in question was acquired by
the Department of the Interior, Bureau of Land Management, in
1944, and that the same was transferred to the Bureau of
Reclamation in 1945.

The land in question was acquired by the Department of the
Interior, Bureau of Land Management, in 1944, and was
transferred to the Bureau of Reclamation in 1945. The
land was acquired by the Department of the Interior, Bureau
of Land Management, in 1944, and was transferred to the
Bureau of Reclamation in 1945.

The land in question was acquired by the Department of the
Interior, Bureau of Land Management, in 1944, and was
transferred to the Bureau of Reclamation in 1945. The
land was acquired by the Department of the Interior, Bureau
of Land Management, in 1944, and was transferred to the
Bureau of Reclamation in 1945.

The land in question was acquired by the Department of the
Interior, Bureau of Land Management, in 1944, and was
transferred to the Bureau of Reclamation in 1945. The
land was acquired by the Department of the Interior, Bureau
of Land Management, in 1944, and was transferred to the
Bureau of Reclamation in 1945.

The land in question was acquired by the Department of the
Interior, Bureau of Land Management, in 1944, and was
transferred to the Bureau of Reclamation in 1945. The
land was acquired by the Department of the Interior, Bureau
of Land Management, in 1944, and was transferred to the
Bureau of Reclamation in 1945.

COMMISSION 4

ON THE MAGNETOSPHERE

Prof. K.L. Bowles, Chairman

Session	Pages
4/3 = 3/4 IONOSPHERE THEORY (Joint with Commission 3) 0900 Wednesday, 11 September ROOM 307RB See Commission 3 Program	47 - 51

Commission 4 regularly has a full schedule at the USNC-URSI Fall Meeting, but has regretfully limited itself to this one joint session with commission 3 as a result of the pressure of too many closely spaced meetings dealing with the magnetosphere.

US Commission 5 does not regularly hold sessions at the fall USNC-
meeting.
URSI US Commission 7 does not schedule sessions at these meetings.

COMMISSION 6

RADIO WAVES AND TRANSMISSION INFORMATION

Dr. R.C. Hansen, Chairman

Session	Pages
6-1 SCATTERING 1400 Tuesday, 10 September Room 455EC Chairman: J. Crispin KMS Industries Ann Arbor, Michigan 48106	75-79
6/2 = 2/6 -1 ROUGHNESS AND OTHER EFFECTS RELATED TO THE SURFACE OF THE EARTH (Joint with Commission 2) 0900 Wednesday, 11 September Room 356EC See Commission 2 Program	21-25
6-2 PLASMAS 1400 Wednesday, 11 September Room 455EC Chairman: Dr. R. Kodis NASA Electronics Research Center Cambridge, Mass. 02138	81-86
→ 6-3 ANTENNAS 0900 Thursday, 12 September Room 307RB Chairman: Dr. J. Dyson Antenna Laboratory University of Illinois Urbana, Illinois 61801	88-92
6-4 ELECTROMAGNETIC THEORY 0900 Thursday, 12 September Room 309RB Chairman: Dr. R. Kouyoumjian Electroscience Laboratory Ohio State University Columbus, Ohio 44117	93-98
6/1 = 1/6 -1 ANTENNA MEASUREMENTS (Joint with Commission 1) 0900 Thursday, 12 September Room 455EC See Commission 1 program.....	3-6
Business Meeting Immediately Following Session 6-2 approx 1730	87

2

6

CONFIDENTIAL

MEMORANDUM FOR THE DIRECTOR

DATE: 11/11/54

TO:

FROM:

SUBJECT: [Illegible]

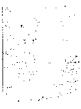
[Illegible text]

[Illegible text]

[Illegible text]

[Illegible text]

[Illegible text]



SCATTERING

J. Crispin, Chairman

6.1-1 NUMERICAL SOLUTION OF THE EXTERIOR SCATTERING PROBLEM AT EIGEN-FREQUENCIES OF THE INTERIOR PROBLEM. K. M. Mitzner, Northrop Norair, Hawthorne, California

The problem of scattering from a perfect conductor of complex shape can be treated by formulating it in terms of an integral equation and then solving the equation numerically. In most cases this approach yields good results for exterior scattering problems. However, if we are at an eigen-frequency of the related interior problem, then the numerical solution obtained by standard means usually bears little relation to the true solution.

We present here a simple, mathematically sound, and highly practicable method for overcoming this difficulty. The basic idea is to combine the standard second kind integral equation

$$\left(\frac{1}{2} I - L\right) \cdot \underline{K} = \underline{K}_e^{inc} \quad (I)$$

and the standard first kind equation

$$M \cdot \underline{K} = \frac{1}{Z_0} \underline{K}_m^{inc} \quad (II)$$

into a new second kind equation

$$\left(\frac{1}{2} I - L + \alpha \underline{n} \times M\right) \cdot \underline{K} = \underline{K}_e^{inc} + \alpha \frac{1}{Z_0} \underline{n} \times \underline{K}_m^{inc}, \quad 1 \geq \alpha > 0. \quad (III)$$

Here \underline{K} is the surface current induced on the scatterer, \underline{K}_e^{inc} and \underline{K}_m^{inc} are source terms, and L and M are dyadic integral operators; I is the identity operator, Z_0 the free space wave impedance, and \underline{n} the outward unit normal.

If α is chosen sufficiently large, (III) can be used for computation at all frequencies with no special precautions. This observation is confirmed both by theoretical considerations and by actual numerical results.

Analogous methods can be used to remove the corresponding difficulty in both the hard and soft problems of scalar scattering.

* This work was supported by the Air Force Avionics Laboratory, Wright-Patterson Air Force Base, under Contract F 33615-67-C-1843.

6.1-2 A COMPARISON OF NUMERICAL METHODS FOR THIN WIRE ANTENNAS. A. R. Neureuther, B. D. Fuller, G. D. Haake, G. Hohmann, C. C. Hung, H. A. Kalhor, B. R. Kendall, A. D. Kreiss, J. P. Scherer, A. P. Shomo, T. C. Tong. Department of Electrical Engineering and Computer Sciences and the Electronics Research Laboratory, Students in the graduate antenna course. Department of Electrical Engineering and Computer Sciences, University of California, Berkeley

A number of numerical techniques have been developed for analyzing antenna and scattering problems involving thin wires. There are at least three popular integral equations, two philosophies as to the expansion of the unknown and the variety of methods for interpolating in the uses of one of these expansions. Although basic arguments can be made as to which approach should be the best in a given situation, to date there has been a lack of data for comparison purposes.

The generation of such data in hopes of establishing quantitative comparisons was undertaken as a class project in the graduate antenna course in the Department of Electrical Engineering and Computer Sciences at the University of California at Berkeley. A total of eight different approaches were used to analyze half and full wave dipole antennas and scatters. The results for the accuracy and computation time quantitatively support the following conclusions.

1. The expansion of the unknown current in functions of subrange support rather than full range support greatly reduces the integration time and hence the computation time.
2. The use of quadratic or sinusoidal interpolation permits roughly a factor of three reduction in the matrix size for the same accuracy.
3. The use of Pocklington's integral equation requires approximately three times the matrix size to produce the same accuracy as that obtained with the use of Hallen's integral equation.

[†]Subsidized computer time provided by the University of California through the Berkeley Computer Center.

6.1-3 WAVE PROPAGATION IN AN OPEN, PERIODIC, TWO-DIMENSIONAL IRIS WAVE-GUIDE. Gary S. Brown, HG, ISG USACDCEC, Fort Ord, California 93941, Raj Mittra, Department of Electrical Engineering, University of Illinois, Urbana, Illinois 61801

The existence and character of modal fields on a structure consisting of an infinite series of slotted metal planes is considered. No variation in one transverse coordinate is assumed. Integral equations involving the unknown field in one iris and the propagation constant are formulated for both types of polarization with the aid of appropriate Green's functions. The integral equations are reduced to infinite matrix equations via the application of Galerkin's method in the Fourier transform domain. The so-called odd and even radial Mathieu functions of the first kind are found to yield a rapidly convergent series representation for the iris field and the appropriate polarization. Individually, these particular functions satisfy the required boundary conditions thus giving a consistent representation for the iris field.

For a given polarization, the first two modal propagation constants and slot field distributions are computed for even field symmetry. The real or attenuating part of the propagation constant is found to oscillate between a maximum and a minimum value as a function of the distance between adjacent planes when this distance is large compared to the iris width. The field distribution in the iris is also found to be very insensitive to plane spacing but becomes more peaked as the iris width is increased.

6.1-4 MULTIPLE SCATTERING OF ELECTROMAGNETIC WAVES BY DIELECTRIC AND METAL SPHERES. J. H. Bruning and Y. T. Lo, Antenna Laboratory, University of Illinois, Urbana, Illinois 61801

An exact solution, in series form, to the problem of multiple scattering of E.M. waves by two spherical bodies is available through use of the translational addition theorem for vector spherical wave functions. As demonstrated by Liang and Lo, there are some severe restrictions in this method in regard to obtaining numerical results when sphere radius is larger than about $\lambda/3$. This is due primarily to the difficulty of computation of the Wigner 3-j coefficients which appear in another set of coefficients. A stable three term recursion relation for these latter coefficients along with starting values has been derived, thereby eliminating the need to calculate 3-j coefficients. With this simplification and several others obtained through symmetry, a very fast program has been written for the calculation of the fields scattered by two spheres of dielectric and/or conductive material. With this method, computation is now practical for spheres of radius as large as several wavelengths. This provides a good method to check the validity and range of the modified geometric diffraction theory approach

described by Bruning and Lo. The translational approach, of course, must be used for very small spheres, but is limited in the case of very large spheres only by computation time. For large metallic spheres, the geometric diffraction approach is preferred. There is good agreement between these two methods for spheres of radius ranging from $\lambda/3$ to several wavelengths.

The results of these two methods, together with an asymptotic form of the translational approach for large separation, will be compared with some experimental work recently performed by the author. Included in the series of scattering measurements are some rather interesting results involving back-scattering by a conducting and dielectric sphere in close proximity. The agreement with theory is quite good.

6.1-5 DIFFRACTION BY SMOOTH CONVEX SURFACES. Soonsung Hong, M.I.T. Lincoln Laboratory, Lexington, Massachusetts

This paper describes an asymptotic method of obtaining the far-field expression for diffraction of plane waves by a smooth body (e.g. spheroids, elliptic cylinders). The asymptotic method previously available was that proposed by Levy and Keller,¹ which treats diffracted waves as disturbances following geodesics and, furthermore, assumes that the only relevant curvature is that in the direction of the geodesic. Using their method, it is difficult to find higher order terms which show the effect of curvature in the direction transverse to the geodesic.

The present analysis is based on the asymptotic method of solving the integral equation. Using the solution for the induced surface fields which was derived in a previous paper,² the integral equation governing the far fields is solved. The leading and second-order terms in the asymptotic expansion of the diffracted fields are explicitly obtained, and the effects of curvature along and transverse to the geodesic ray paths are discussed. When the curvatures are constant (or when the transverse curvature is zero) the results reduce to the asymptotic forms of the exact series solutions for the sphere (or the cylinder). For a prolate spheroid, the theoretical estimation agrees with experimental data even in resonance region.

* Operated with support from the U. S. Advanced Research Projects Agency

1. B. R. Levy and J. B. Keller, "Diffraction by a Smooth Object," *Comm. Pure and Appl. Math.*, Vol. 12, pp. 159-209.
2. S. Hong (1959) "Asymptotic Theory of Electromagnetic and Acoustic Diffraction by Smooth Convex Surfaces of Variable Curvature," *Journal of Math. Phys.*, Vol. 8, No. 6 pp. 1223-1232 (June 1967).

6.1-6 MODIFIED SINGLE DIFFRACTION. J. Freehand

In the two-dimensional problem of the perfectly-conducting strip, let the incident magnetic vector be parallel to the edges.

The geometrical theory of diffraction leads to a solution for the far zone field which is the sum of two phenomena:

- 1) Single diffraction, given by two terms.
- 2) Multiple diffraction, given by four terms, each of which is actually an infinite series written in closed form.

Four different solutions have appeared in the literature. The two singly-diffracted rays are always the same; construction of the multiply-diffracted rays varies according to the way each author uses the diffraction coefficients. Each of the four solutions is defective in a characteristic way; not one satisfies all of the following desired conditions for the far zone field:

- 1) Planar and normal symmetry.
- 2) Reciprocity.
- 3) Error is independent of angles of incidence and diffraction; i.e., the error is a function of strip width alone.

In order to eliminate multiple diffraction, single diffraction has been modified to meet the above conditions. The modification is based on a comparison of the formula for single diffraction with the formula obtained when the physical optics approximation is used for the strip current. It is found that Fresnel integrals are needed.

The well-known difficulties (of the singly-diffracted ray solution) for near-grazing incidence vanish. Graphical accuracy might lead one to think that modified single diffraction is an exact solution for strips greater than one-half wavelength in width.

0900 Wednesday, 11 September

ROOM 356EC

ROUGHNESS AND OTHER EFFECTS RELATED TO THE SURFACE OF THE EARTH

[See Commission 2 Program]

2

6

PLASMAS

R. Kodis, Chairman

6.2-1 IMPEDANCE OF A PARALLEL PLATE CAPACITOR IN A COMPRESSIBLE, INHOMOGENOUS, COLLISIONAL MAGNETO-PLASMA. Hi Dong Chai, Northeastern University, Boston, Massachusetts

A qualitative study of impedance of a section of an infinitely large parallel plate capacitor in plasma is presented using macroscopic hydrodynamic equations.

First starting from the definition of impedance (ratio of voltage to current), an impedance formula is derived as an integral of first order normalized velocity function. This reduces the problem into one of finding the normalized velocity which is a solution to an ordinary, inhomogenous second order differential equation. Secondly, the impedance of the capacitor in a homogenous, compressible, collisional magneto-plasma is obtained. Effects of collision, uniform magnetic field and capacitor plate separation are graphically presented using the homogenous plasma.

For the inhomogenous compressible plasma a difference method is used to obtain the impedance. The effect of the sheath is presented in a graphical form for the cold plasma and in a tabular form for the compressible plasma.

A possibility of using the impedance variation of a homogenous cold plasma around the plasma frequency in diagnosing the electron density and collision frequency is pointed out.

In this study the ion motion is neglected. The adiabatic law which relates pressure to electron density and the totally-reflecting boundary condition are applied.

6.2-2 MODE COUPLING IN A COMPRESSIBLE ISOTROPIC TURBULENT PLASMA. R. E. Collins, Division of Electrical Sciences and Applied Physics, Case Western Reserve University, Cleveland, Ohio 44106

Propagation of plane electromagnetic waves in random dielectric media has been analyzed by many authors using perturbation methods.¹⁻⁴ Such methods have also been applied to obtain the dispersion relation for plane waves in a cold anisotropic plasma by Liu.⁵ In this paper, Keller's perturbation theory is used to obtain the dispersion relation for plane waves in a compressible fluid-like isotropic plasma.⁶

6

The plasma under study is considered to have a turbulent character which is predominantly that of the neutral gas, i.e., the plasma is weakly ionized and the electrons and ions have a random spatial variation in density, velocity, temperature, and pressure, which is induced by the turbulence in the neutral gas. For a uniform isotropic plasma, there are two independent modes of propagation, the transverse electromagnetic mode, and the longitudinal acoustic-like mode. Spatial gradients in the electron density will couple these modes together. For essentially the same reasons a random spatial variation in density, pressure, etc. couples these pure transverse and longitudinal modes together and gives rise to two modified modes, which are not pure transverse or longitudinal, and with modified propagation constants.

In this paper, the dispersion relation, accurate to second order in the degree of randomness, is derived in terms of appropriate correlation functions. Specific results for the degree of coupling, change in propagation constant, and the attenuation rates, will be given for the case when the correlation functions correspond to those for a multivariate Gaussian Distribution.

6.2-3 THE EQUIVALENT REYNOLDS NUMBER AND SPECTRAL EXTENT OF PLASMA TURBULENCE. James T. Coleman, PhD. Battelle Memorial Institute, Columbus Laboratories, Columbus, Ohio 43201

The nature of ion-acoustic wave induced plasma turbulence is of interest to radio experimenters as it can be the cause of certain modulations and distortions of signal transmissions through the ionosphere. The paper describes prediction of the onset of this type of turbulence in terms of an equivalent Reynolds number. A simplified graphical technique is given for the estimation of this quantity for a number of plasmas of interest. The paper also describes prediction of the extent of the turbulence spectrum in wave number space in terms of the orientation of an applied magnetic field. Experimental evidence is presented for the variation of the threshold and the measured spectral width of the turbulence spectrum for arbitrary magnetic field magnitudes and orientations.

The marginal stability boundaries of Dougherty¹ are compared with the stationary turbulence calculations of Ichimaru.² Both of these studies were performed in the hydrodynamic approximation and thus direct comparisons are permissible. Areas of qualified agreement and disagreement are discussed in detail. A previous URSI paper³ described the agreement between the experimental work of Coleman, the marginal stability boundaries of Dougherty, and the turbulence spectra of Ichimaru. The present paper expands this work to permit extension to the more general case of electron drift in a direction not aligned with the externally applied magnetic field.

It is demonstrated from theory and experiment that the onset of and

spectral content of ion-acoustic wave turbulence is modified by the magnitude and spatial orientation of an externally applied magnetic field. The sensitivity to variation of this field is also considered briefly.

References:

1. J. P. Dougherty, "The Conductivity of a Partially Ionized Gas in Alternating Electric Fields", *J. Fluid Mech.*, 16, 126-137 (1963).
2. Ichimaru, S. and Nakana, T., "Theory of a Turbulent Stationary State of a Plasma", *Phys. Rev.*, 165, 1, 231-250, January 1968.
3. Coleman, J. T., "On the Anomalous Behavior of the Spectra of Ion-Acoustic Wave Induced Plasma Turbulence", Commission 6, Paper 3-3, 1968 URSI Spring Meeting, Washington, D.C., April 1968.

6.2-4 ELECTROMAGNETIC WAVE PROPAGATION IN A DIELECTRIC MEDIUM SPACE-TIME MODULATED BY A NON-LINEAR PUMP WAVE. B. Rama Rao, Gordon McKay Laboratory, Harvard University, Cambridge, Massachusetts 02138

During the last few years several authors^{1,2} have considered the propagation characteristics of electromagnetic waves travelling in media with properties varying periodically in time and space. In all of these cases, it is tacitly assumed that the perturbing wave modulating the medium is a weak, progressive, sinusoidal disturbance. However, there are many physical applications in ultrasonics³, quantum electronics⁴, and in plasma⁵ and ionospheric physics where the modulating pump wave has a large amplitude and contains several harmonics of the fundamental pumping frequency. Electromagnetic wave propagation in dielectric media of this type is analyzed in this paper.

It is assumed that the high intensity pump wave (either acoustic or microwave phonon wave) travelling along the z direction in an infinite dielectric medium contains two pump harmonics and causes the dielectric constant of the medium to vary in the following manner:

$$\epsilon(z, t) = \epsilon_0 + \epsilon_1 \cos(\omega_v t - k_v z) + \epsilon_2 \cos(2\omega_v t - 2k_v z)$$

where $\epsilon_2 \ll \epsilon_1 \ll \epsilon_0$. ω_v and k_v are the angular frequency and wave number of the fundamental component of the pump wave. To keep the analysis simple only the first two pump harmonics are considered. A dispersion relation in the form of continued fractions involving all space-time harmonics has been obtained for electromagnetic wave propagation in an infinite dielectric medium. The convergence criterion has been established from Poincare's theorem and a 'sonic' region has been defined. The physical

parametric processes involved are explained in terms of equivalent 'Non-linear Polarization Sources' postulated by Bloembergen⁶. The second harmonic modulating coefficient ϵ_2 causes parametric coupling between the first-order Stokes and Antistokes waves. The theory developed here is used to explain some experimental observations on the non-linear scattering of microwaves by large amplitude, electron-density fluctuations in plasmas.

References

- (1) A. Hessel and A. A. Oliner, IRE Trans. MTT-9, 1961, pp. 337-343.
- (2) S. T. Peng and E. S. Cassedy, Symposium on Modern Optics, Polytechnic Press, 1967.
- (3) I. G. Mikhailov and V. A. Shutilov, Soviet Physics - Acoustics, Vol. 5, 1959, pp. 75-78.
- (4) R. G. Brewer, Applied Physics Letters, Vol. 5, 1964, p. 86.
- (5) B. Rama Rao and W. A. Saxton, "Bragg Scattering by Moving Striations in a Plasma Column", 1968 Spring URSI meeting, Washington, D.C.
- (6) N. Bloembergen, "Non-Linear Optics", New York: W. A. Benjamin & Co., 1965.

6.2-5 IMPEDANCE VARIATIONS OF A MONOPOLE ANTENNA PASSING THROUGH A SATELLITE'S WAKE. R. G. Yorks, H. Weil, W. H. Potter, University of Michigan - Radio Astronomy Observatory, Ann Arbor, Michigan

The University of Michigan - Radio Astronomy Observatory experiment on the NASA Orbiting Geophysical Observatory-II (OGO-II) satellite was provided an unexpected opportunity to assess the effects of a spacecraft wake on the measured impedance of a monopole antenna. The original purpose of the experiment was to map the cosmic background with a 2.5 MHz radiometer by means of ionospheric focusing. A 2.5 MHz impedance bridge was included to continuously measure the complex impedance of the 18.3 meter monopole antenna.

OGO-II, although intended to be a fully stabilized spacecraft in a near polar orbit, went into spin stabilized operation after ten days operation. A favorable spin axis orientation carried our antenna through the wake, out in front of the spacecraft and back into the wake every four to nine minutes. During intervals around perigee, when

the plasma, gyro and operating frequencies of the unperturbed ionosphere, ω , ω_p and ω_c apparently satisfy $\omega_p^2 > \omega^2 - \omega_c^2$ and $\omega < \omega_c$, very marked variations occur in the observed antenna impedance. The observed effects are interpreted as due to the changing angles of antenna to wake and antenna to magnetic field.

Information gained from studying the OGO-II data will be used for studying some characteristics of the wake structure, and the empirically observed impedance variations will be used in interpreting our OGO-IV data. OGO-IV is fully stabilized and carries an experiment identical to that on OGO-II.

This work was supported by the National Aeronautics and Space Administration under Contract NAS5-3099.

6.2-6 SCATTERING BY A CONDUCTING CYLINDER COATED WITH A MOVING PLASMA SHEATH. C. Yeh, Department of Engineering, University of California, Los Angeles, California 90024

The problem of the scattering of electromagnetic waves by plasma coated cylinder is not only of interest from a theoretical point of view but also possesses a very important application, i.e., the understanding of the re-entry problem. Most previous theoretical analysis were carried out with the assumption that the scattering cylindrical object was coated either with an inhomogeneous plasma sheath¹, an anisotropic plasma sheath² or an anisotropic and inhomogeneous sheath³. At no time was the plasma sheath assumed to be moving with respect to the conducting cylinder or an observer. It is well known that the plasma surrounding a re-entry vehicle is moving with respect to an observer. The purpose of this investigation is to consider this interesting problem. Specifically, we shall obtain the scattering characteristics of a plane wave incident upon a conducting cylinder coated with a homogeneous plasma sheath which is moving in the axial direction with a uniform velocity V_0 with respect to the conducting cylinder. This problem provides another interesting application for the study of the interaction of electromagnetic waves with moving media.

Solutions of this problem are obtained by making use of the special theory of relativity, the covariance of Maxwell's equations, and the Lorentz transformations⁴. To qualitatively illustrate how the solutions behave, the radiation patterns of the scattered fields and the backscattering cross sections are computed. Numerical results show that the radiation patterns and the backscattering cross sections are rather sensitive functions of V_0 , the velocity of the moving plasma sheath. Furthermore, a rather unique feature concerning mode coupling between the incident wave and the scattered wave is found. Even at normal incidence for $V_0 \neq 0$, an incident TE wave

will produce a scattered wave which contains both TE and TM modes. Detailed discussions will be presented.

¹J. R. Wait, "Electromagnetic Waves in a Stratified Media", Pugamon Press, New York (1962).

²H. C. Chen and D. K. Cheng, IEEE Trans. on AP-12, 348 (1964).

³W. V. T. Rusch and C. Yeh, IEEE Trans. on AP-15, 452 (1967).

⁴C. Möller, "The Theory of Relativity", Oxford University Press, London (1957).

6.2-7 MONITORING THE IONOSPHERE BY MEANS OF HF FREQUENCY MEASUREMENTS.

Kurt Toman and Albert H. Lorentzen, U. S. Air Force Cambridge Research Laboratories, L. G. Hanscom Field, Bedford, Massachusetts

Assuming that ionospheric phase paths exist, ionospheric variations are studied by measuring continuously and simultaneously the frequencies of two HF radio emissions (3.330 and 7.335 MHz) as received via the ionosphere. Although transmitters and receivers are separated by a fixed earth-surface distance of 475 Km (CHU-Ottawa, Canada; AFCRL-Bedford, Mass.) the received frequencies of the ionospheric transmissions vary with time in accordance with Doppler's principle. These frequency shifts are usually brought about by naturally induced ionospheric variations.

Frequency recordings are made on magnetic tape. The data is processed and displayed by means of a Ray Span Analyzer. Mode separation in the frequency domain is illustrated. The ratio of phase path velocities reveals at times the nature of the ionospheric motion. Analog and digital integration techniques are used to obtain phase path variations with good resolution.

1730 Wednesday, 11 September

ROOM 455EC

BUSINESS SESSION FOR COMMISSION 6

6

ANTENNAS

J. Dyson, Chairman

6.3-1 DESIGN OF DUAL-REFLECTOR (CASSEGRAINIAN TYPE) ANTENNAS. F. Rouffy, Advanced Sensors Laboratory, Research and Development Directorate, U. S. Army Missile Command, Redstone Arsenal, Alabama 35809

This paper reviews the general design criteria for dual-reflector (Cassegrainian type) microwave large aperture antennas and includes recent developments for the design of ultra-low sidelobe level dual-reflector antennas. Dual-reflector antennas are similar in appearance to Cassegrainian antennas. However, instead of being simple hyperbolic-parabolic conic surfaces of revolution, the dual-reflector surfaces are described by transcendental equations. The transcendental equations, four non-linear differential equations in four unknowns, are stated in terms of the feed horn pattern and the main reflector illumination function. Solution of the design problem consists of selecting a practical surface configuration from the multi-parameter solutions of the design equations.

The special case of uniform amplitude and phase i.e., 100% theoretical efficiency, has been previously considered. This previous work includes summaries of the theory and measurements of dual-reflector antennas which were designed for 100% efficiency, yet which with subreflector blockage and diffraction effects, attained only 80% antenna efficiency.

The special case considered in this paper is that of the low sidelobe, potentially low-noise dual-reflector antenna. These designs are compared with the maximum efficiency, high sidelobe dual-reflector antennas. In particular, the low sidelobe design technique introduces Taylor-nth-power criteria into the system of four equations in four unknowns. Comparisons are made between the characteristic features of the families of solutions for the two special design cases.

6.3-2 COMMUNICATIONS, RADAR, BROADCASTING LOW-SIDELobe NONSYMMETRICAL BINARY CORPORATE FEEDS FOR HIGH-POWER PHASED ARRAYS. K. G. Schroeder, TRW Systems, Redondo Beach, California 90278

In receiving arrays, a sidelobe-reducing amplitude taper can relatively easily be implemented by the use of attenuators inserted in the feed lines leading from the output ports of regular symmetrical corporate feed structures to the antenna elements. If an amplifier is used at each element (or a mixer and an amplifier), then both with receiving and transmitting arrays the desired amplitude taper can be applied either by

varying the gain of the amplifiers or, in the case of transmitting arrays, by varying the power level at the input to the final amplifiers.

This paper describes efficient antenna array feed networks which generate low-sidelobe amplitude tapers across arrays of either uniformly or non-uniformly spaced elements. These feed networks use two-way hybrid power dividers with equal in-phase outputs, and can thus be designed (depending on frequency) for bandwidths of up to 10:1.

The amplitude taper is achieved by cascading the two-way hybrids nonsymmetrically, so that different power levels appear at the outputs of the total networks. When, for example, the feed network and antenna array is being used in the transmit mode, the transmitter power output is to a first-level hybrid, one output of which is to and through at least one more hybrid than the other output of the first-level hybrid, before ultimate connection to array elements. Further, the next level hybrid may in turn have one of its outputs also connected to and through at least one more power divider, and this can be extended through further division steps in cascade fashion. With the nonsymmetrical binary feed networks thus created, the feed path of least signal power division is connected to a center array element (or elements). Signal power feed paths of progressively more signal power division steps and progressively lower signal power levels are connected to array elements positioned progressively outward from the center array elements.

The types of amplitude papers possible by this method are analyzed in detail, and beam patterns for various types of cascading and various element numbers are determined both by Fourier transform method and direct computer addition.

Finally, impedance matching by means of second-level complementarization is discussed, and practical array networks are described, emphasizing simplicity of design and uniformity of sidelobe level reduction. As an example, a feed network is shown for a proposed 500 KW HF broadcast array with -20 db first sidelobe levels.

The circuit diagram and performance results are shown for a novel step-up hybrid design utilized in this feed network.

References:

- [1] K. G. Schroeder, J. C. David, "On the Averaging of Reflection Coefficients in 180-Degree Hybrid Tees," pp. 626-627, Proceedings of the IEEE (Correspondence), June 1965.
- [2] K. G. Schroeder, "Linear Broadside Arrays of Complementary Pair Elements Groups," 1965 URSI Fall Meeting, Oct. 3-7, Dartmouth College, Hanover, New Hampshire.

- [3] K. G. Schroeder, J. C. David, R. C. Fenwick, "Study Program Leading to the Development of a High-Gain, Broadband Steerable-Beam, High-Frequency Receiving Antenna for the USIA," (Two Volumes), Final Engineering Report on Contract No. IA-10146, Collins No. 523-0556652-001 D3M.

6.3-3 RESONANT END-FIRE RADIATION BY DIELECTRIC COVERED APERTURES.

Elliott R. Nagelberg, Bell Telephone Laboratories, Inc., Whippany, New Jersey

This paper discusses certain effects of a covering dielectric sheath on the far-zone radiation pattern of an aperture bounded by a perfectly conducting ground plane. A significant effect is found to be a broadening of the radiation pattern in a narrow band centered about that frequency at which a surface wave would begin to propagate along a grounded dielectric slab. The results of this broadening are to produce (1) a sharp increase in the power radiated in a direction perpendicular to the aperture (the end-fire direction) and (2) a corresponding dip in the broadside power of a matched aperture, as required by energy conservation. This phenomenon must be distinguished from what is generally referred to as a "surface wave" in that it is a radiative phenomenon rather than a discrete mode of propagation guided by the dielectric sheath. The field thus exhibits an inverse power law variation with distance from the aperture. Furthermore, the end-fire signal amplitude varies symmetrically about a center frequency and therefore does not have a well defined cut-off characteristic.

The theoretical analysis is carried out by a Fourier transform method, from which the far-zone field is determined by a saddle point approximation. In order to corroborate the theoretical results, measurements will also be given of end-fire and broadside radiation as a function of frequency.

➤ 6.3-4 REMOVAL OF BLINDNESS IN PHASED ARRAYS. V. D. Agrawal and V. T. Lo, Antenna Laboratory, University of Illinois, Urbana, Illinois 61801

It is well known that mutual couplings in phased antenna arrays can cause blind regions in the scanning characteristic of the array. This paper describes a method of designing the arrays which can be used for scanning over a wide angle without any blind regions.

As pointed out by several authors [1], the blindness regions are caused by the linear dependence of mutual coupling phase upon the distance between the antennas. In the arrays of uniform spacings, this results in the accumulation of couplings in certain scanning directions. This accumulation can be avoided by using nonuniform spacings between

the elements. In particular, we have considered the random arrays [2]. Element pattern approach [3] has been used to determine the scanning characteristic, and the probabilistic property of the main beam amplitude of the array as a function of scanning angle is obtained. It was found that the blind regions were completely eliminated. It is also shown that the statistical results can be used for large arrays with greater confidence. To illustrate the practicability of such arrays, an example is given. Although the array considered in this example is not very large (51 elements), the blind regions in its scanning characteristic were found to be totally absent.

References

- [1] L. W. Lechtreck, "Effects of Coupling Accumulation in Antenna Arrays," IEEE Trans. Antennas and Propagation, Vol. AP-16, pp. 31-37, January 1968.
- [2] Y. T. Lo, "A Mathematical Theory of Antenna Arrays with Randomly Spaced Elements," IEEE Trans. Antennas and Propagation, Vol. AP-12, pp. 257-268, May 1964, and "An Experiment on the Antenna Arrays with Randomly Spaced Elements," IEEE Trans. Antennas and Propagation, Vol. AP-15, pp. 231-235, March 1967.
- [3] A. A. Oliner and R. G. Malech, "Mutual Coupling in Infinite Scanning Arrays," Microwave Scanning Antennas, edited by R. C. Hansen, Vol. II, Chapter 3.

6.3-5 CHARACTERISTICS OF DIELECTRIC COVERED AND LOADED CIRCULAR WAVEGUIDE PHASED ARRAYS. Noah Amitay and Victor Galindo, Bell Telephone Laboratories, Whippany, N. J.

Many significant characteristics of dielectric-free circular waveguide phased arrays have been discussed previously for both hexagonal¹ and rectangular² grids excited by linear and circular incident polarizations. The method of analysis,¹ an application of the Ritz variational procedure, is readily applicable to the analysis of the same arrays when they are covered, loaded or plugged with dielectric materials. The effects of the dielectrics on the impedance and radiation properties of the array have been studied and the numerically obtained results closely agree with experimental results.

For various hexagonal grids the effects of dielectric sheaths (covers) and plugs as a function of their thicknesses and dielectric constant were studied. Fully loaded waveguides were also studied as a function of the electrical and geometrical parameters.

Three types of forced surface waves were observed. One type exists in the absence of dielectrics, and its location (with scan) shifts towards broadside with increasing dielectric constant. A second type of surface wave is "trapped" in the dielectric over and requires a minimum sheath thickness for propagation, whereas the third type of surface wave is "trapped" in dielectric plugs and propagates only for certain ranges (pass bands) of plug thickness. In contrast to conclusions reached by other investigators,³ it is found that forced waves occur at isolated beam pointing directions.

1. N. Amitay and V. Galindo, "The Analysis of Circular Waveguide Phased Arrays," present at the Spring, 1968 ISRU meeting, Washington, D.C., to be published in the Bell System Technical Journal.
2. N. Amitay and V. Galindo, "A Note on the Radiation Characteristics and Forced Surface Wave Phenomena in Triangular-Grid Circular Waveguide Phased Arrays," to be published.
3. R. F. Frazita, "Surface-Wave Behavior of a Phased Array Analyzed by the Grating-Lobe Series", IEEE Trans. on Antennas and Propagation, Vol. AP-15, No. 6, November 1967, pp. 823-824.

6.3-6 MEASUREMENTS OF STOKES PARAMETERS FOR MICROWAVE LINE SPECTRA.

Wm. A. Coles, V. H. Rumsey, W. J. Welch, University of California, La Jolla, California

To measure the polarization of an extensive cosmic source one needs an antenna that would, when transmitting, produce the same polarization in very direction within its beam, for a variety of polarizations. Polarimeter designs that approximate this in the microwave range will be described. Calibration procedures will be described which yield the Stokes parameters from any four distinct antenna polarizations independently of instrumental error.

The observational procedure is considered with regard to radiometer gain stability, efficiency in maximizing integration time, and providing redundancy without loss of efficiency. The integration times given each observation are weighted according to a rather flexible criterion.

The handling of raw spectrometer data will be described. This includes the removal of systematic effects such as offsets and differential gains; the extraction of Stokes parameter spectra; the consistency checks; and the fitting of a model to these spectra.

It is a pleasure to acknowledge partial support from the National Science Foundation for this work.

ELECTROMAGNETIC THEORY

R. Kouyoumjian, Chairman

6.4-1 ON THE WIENER-HOPF TECHNIQUE IN TWO COMPLEX VARIABLES. N. H. Kuo and M. A. Plonus, Northwestern University, Evanston, Illinois

The object of this paper is to show that considerable simplification can be achieved by formulating diffraction problems in the sense of the theory of distributions and that there is a procedure of solving Wiener-Hopf equations without performing a product factorization. The problem, diffraction by a right-angled dielectric wedge, is chosen for displaying these ideas. The analysis, an extension of earlier work of the authors,¹ is in essence a generalization of the Wiener-Hopf technique from one to two complex variables.

The field behavior at the corner of the wedge is examined. Numerical results are included, which show that the solution in a form of infinite series converges very slowly. It appears that we can improve the technique by using a suitable set of basis functions. This will be investigated in a sequel to this work.

1) N. H. Kuo and M. A. Plonus, "A Systematic Technique in the Solution of Diffraction by a Right-Angled Dielectric Wedge" J. Of Math. and Phys., vol. 46, pp. 394-407, Dec. 1967.

6.4-2 INTEGRAL EQUATION SOLUTIONS FOR THE RADIATION FROM A WAVEGUIDE THROUGH A DIELECTRIC SLAB. C. P. Wu, Bell Telephone Laboratories, Inc., Whippany, N. J. 07981

The radiation from a waveguide covered by a dielectric slab has received considerable attention recently.¹ The properties of such antennas depend upon the aperture field distribution, which in turn is determined by the various parameters, such as the waveguide width in terms of wavelength, the dielectric constant, and the slab thickness. The problem, however, has hitherto been treated only approximately in that the incident wave is assumed for aperture field in the variational calculation of the radiation impedance. The adequacy of this approach has yet to be fully verified.

In this paper, we attack the problems directly by using the

integral equation formalism. The integral equation of the present problem differs from those which commonly appear in scattering theory in a very important respect, namely its kernel contains a continuous spectral representation which seems most conveniently expressed in the form of Fourier integrals. By judicious manipulation, however, it is possible to convert such kernels into a form suitable for solution by the method of moments. This procedure thus enables us to determine the true aperture fields accurately. The results show that under certain conditions higher order modes are strongly excited in the aperture and that they should be included in the calculation of radiation impedances and patterns as well as in the determination of surface wave excitation. The inclusion of higher order modes is particularly important in radiation pattern and surface wave calculations, because they have been found to contribute significantly to the excitation coefficients by either enhancing or cancelling the effects of the incident mode. Moreover, it has been found that the energy carried by the surface wave is critically dependent upon the frequency and the characteristics of dielectric slabs.

1. See for example, W. F. Crosswell, R. C. Rudduck, and D. M. Hatcher, "The Admittance of a Rectangular Waveguide Radiating into a Dielectric Slab," IEEE Trans. on Antennas and Propagation, Vol-AP-15, pp. 627-633, September 1967

6.4-3 SOLUTION OF INTEGRAL EQUATIONS OF ELECTROMAGNETIC THEORY BY MEANS OF THE TRANSFORM DOMAIN REPRESENTATION TECHNIQUES. A. R. Neureuther and H. A. Kalhor, Department of Electrical Engineering and Computer Sciences, Electronics Research Laboratory, University of California, Berkeley

The subrange support representation technique (SSRT) which involves the expansion of the unknown in terms of a set of functions which are non-zero only over certain subranges of the range of the integral equation is the popular method of solving integral equations. This technique has the advantage that the integration time is greatly reduced due to the use of functions of subrange support. It also has the ability to efficiently represent the unknown near discontinuities and singularities. However, for large objects the number of unknowns becomes excessive as it requires about five unknowns per wavelength of unknown range even with sophisticated interpolation techniques. One new numerical technique which has been developed in an effort to reduce the unknown density is the transform domain representation technique (TDRT).

The TDRT consists of dividing the unknown function throughout the entire range into a dominant part which can be described by a few unknown constants and a smooth part which can be efficiently represented by a complex Fourier series. The separation into the dominant and smooth parts is intended to remove the undesirable effects of the Gibbs phenomena and its repercussions in the transform domain. The Complex Fourier series

representation is chosen specifically because Fast Fourier transform algorithms exist which permit a tremendous reduction in the integration time. The TDRT is not limited to straight structures as might be suggested from the traditional application of Fourier transform techniques. In fact, the only change for arbitrarily curved structures is that the Fourier transform for the far field is no longer simply related to the complex Fourier series used in the unknown function representation.

The potential advantage of the TDRT is that for large structures it may be more efficient in terms of the number of unknown constants required in representing the majority of information about the solution. A count of the basic machine operations shows that for a fixed number of unknowns the running time of the TDRT is approximately the same as that of the SST. Thus any increased efficiency in the unknown representation is directly translatable into the ability to improve on one or more of the three basic aspects of the numerical approach. 1) problem size, 2) accuracy and 3) computation time. The magnitude of the improvement in the efficiency of the representation has been studied by computing representations of known SSRT solutions for the problem of scattering from a perfectly electrical conducting strip. Results will be presented to document the potential advantages of the TDRT.

Research sponsored by the National Science Foundation under Grant GK-676.

6.4-4 SCATTERING OF DIPOLE RADIATION BY A MOVING, DISPERSIVE DIELECTRIC HALF-SPACE. J. Fred Holmes and Akira Ishimaru, Department of Electrical Engineering, University of Washington, Seattle, Washington 98105

This paper studies the scattering of electric dipole radiation by a moving, dispersive dielectric half-space. The dipole is located in the free space above the dielectric and is assumed to be time harmonic in its rest frame, oriented perpendicular to the interface and moving parallel to it.

Previous work in this area has been confined to the use of a plane wave as a source or a non-dispersive dielectric. However, the use of a physically realizable source such as a dipole yields some interesting results which cannot be arrived at using plane wave excitation.

The problem is solved using integral transform techniques. Integral formulations involving two integrations are obtained for the vector potential in both the free space (region 1) and the dielectric (region 2).

The integrals for region 1 are first evaluated using a double saddle point approximation. This yields expressions for the

6

reflected radiation field in both the rest frame of the dielectric and the rest frame of the source for an arbitrary, dispersive dielectric. It is found that the reflected wave has the same frequency distribution in space as the primary wave; however, the distribution is centered on the source image, and therefore in the rest frame of the dielectric, the primary and reflected waves will differ in frequency everywhere except on the interface and a vertical axis through the dipole.

The integrals for region 1 are also evaluated by performing an asymptotic expansion for one integration and then using the saddle point method to complete the evaluation. This is done for the case of a lossless plasma dielectric and yields, in addition to the reflected wave, expressions corresponding to a lateral wave and a surface wave.

It is found that the criteria for existence of the lateral wave is not modified by the relative motion of the source and dielectric. However, in the rest frame of the dielectric, the frequency distribution in space of this wave differs from that of the primary wave.

The criteria for existence of the surface wave is found to be modified greatly by the relative motion of the source and dielectric. It is found that as the relative velocity is increased, the surface wave ceases to be excited in all directions along the surface. The wave becomes restricted to a wedge shaped region ($0 \leq \text{wedge angle} < 2\pi$) behind the source. The frequency distribution in space of this wave also differs from that of the primary wave.

In addition, it is found that in the rest frame of the source all three waves exhibit the frequency of the source and that the field patterns for each of the waves is distorted in both reference frames by the relative motion. The field pattern distortion is illustrated by showing representative field patterns for different velocities and plasma frequencies.

6.4-5 THEOREMS CONCERNING OPTIMIZATION AND SYNTHESIS OF ANTENNA ARRAYS IN A MOVING MEDIUM. Fung-I Tseng and David K. Cheng, Electrical Engineering Dept.s, Syracuse University, Syracuse, N.Y. 13210

It has been pointed out¹ that, for identical radiating elements with an equal current amplitude, the overall radiation pattern of an antenna array moving with a uniform speed in an isotropic medium is the product of the radiation pattern of a single element in the moving medium and that of an array in which isotropic equi-amplitude point sources replace the

elements in the moving medium. In this paper we shall demonstrate that a simple modification in the phase terms of the element excitations will render the presently available optimization and pattern synthesis techniques useful for arrays in a moving medium.

The analytical formulation will assume that the radiating sources and the observer are stationary in a reference frame and are immersed in a homogeneous and isotropic linear medium which moves with a constant velocity \bar{v} ($v^2 \ll c^2$). The radiation pattern functions for arrays of infinitesimal (point) current sources and of finite linear antennas are given separately, from which the rules for synthesizing a given pattern, or for optimizing the gain or the signal-to-noise ratio of the arrays are obtained and stated in the form of theorems.

¹H. Fujioka and N. Kumagia, "Radiation characteristics of antenna arrays in a moving medium," *Electronics and Communications in Japan*, vol. 49, pp. 100-107, August 1966.

6.4-6 ATTENUATION OF AN ELECTROMAGNETIC WAVE BY A LAMINAR CONDUCTING FOIL IN A WAVEGUIDE. Dr. -Ing, M. R. E. Bichara, Texas Instruments, Dallas, Texas

The measurement of the absorption coefficient or the resistivity of highly resistive thin semiconducting samples ($\approx 10^6$ ohm.cm) cannot be carried out satisfactorily using frequency domain reflectometry owing to the large skin effect depth involved even at microwave or millimeter frequencies.

It is the purpose of this paper to show that an effective way of measuring these parameters is to insert the sample, in the form of a thin foil, inside a waveguide with its large side parallel to the electric field and perpendicular to the plane of polarization when using the TE_{10} -mode of propagation.

Classical electromagnetic theory is used to derive an expression relating the resistivity of a laminar conducting foil to the attenuation undergone by an electromagnetic wave propagating in a rectangular waveguide.

The theoretical procedure consists in deriving Maxwell's equations for a laminar conducting foil placed parallel to the E-plane to obtain the field components present in the sample. Two expressions giving the power absorbed by the sample are obtained and equated to yield a formula relating the attenuation of the wave to the electrical and geometrical parameters of the sample.

Experimentally a special circuit had to be devised to permit the accurate measurement of 0.001 dB with an uncertainty of ± 0.0001 dB and the results obtained fit the theory very well.



6.4-7 REACTIVE-WALL WAVEGUIDE. F. J. Tischer, North Carolina State University, Raleigh, North Carolina

Waveguides with reactive walls have been investigated earlier in connection with the so-called "leaky-wave" antennas. Some of these antennas contain waveguides with one wall replaced by a metallic strip structure or a wire grid which can be considered as reactive walls. The analyses described in the literature were carried out by the "transverse resonance" method applying a "transverse network representation." In some cases, this method of analysis is unsatisfactory. In the present paper, a direct field approach is described which yields accurate relationships for the field distribution, wave modes, and propagation characteristics of the reactive-wall guide.

0900 Thursday, 12 September

ROOM 455EC

ANTENNA MEASUREMENTS

[See Commission 1 Program]



AUTHOR INDEX

Aarons, J.	41	David, M.J.	58
Abraham, L.G.	15	Day, J.W.B.	19
Agrawal, V.D.	90	deBettencourt, J.T.	67
Aitken, G.J.M.	6	Detert, D.G.	44
Akasofu, S.I.	65	Eggers, S.	4
Allen, R.S.	41	Elkins, T.J.	42
Altman, F.J.	17	Fang, D.J.	47
Altschuler, E.E.	19	Fentress, G.H.	8
Amitay, N.	91	Ferraro, A.J.	60
Arendt, P.R.	62	Freeland, J.	79
Barnett, W.T.	28	Fritz, J.	49
Barrington, R.E.	64	Frost, A.D.	42
Barrow, B.B.	15	Fuller, B.D.	76
Barrick, D.E.	24	Fung, A.K.	22
Barsis, A.P.	21	Galejs, J.	50
Beatty, R.W.	8	Galindo, V.	91
Belknap, D.J.	66	Gallant, R.M.	15
Bichara, M.R.E.	97	Garriott, O.K.	58
Birkemeier, W.P.	16	Gassmann, G.J.	60, 63
Bolgiano, R. Jr.	33	Gerks, I.H.	16
Boucher, R.J.	32	Glover, G.H.	7
Broderick, R.F.	22	Glover, K.M.	32
Brown, G.S.	77	Goldberg, B.	67
Bruning, J.H.	77	Gray, D.A.	26
Buchau, J.	65	Grossi, M.D.	52
Burke, G.	5	Haake, G.D.	76
Carlson, A.V.	29	Haggarty, R.D.	66
Chai, H.D.	81	Hardy, K.R.	32
Champlin, K.S.	7	Hayre, H.S.	22
Chang, D.C.	50	Hogg, D.C.	36
Cheng, D.K.	96	Hohmann, G.	76
Clark, R.F.	9	Holm, J.D.	7
Clark, R.R.	42	Holmes, J.F.	95
Clifford, S.F.	26	Hong, S.	78
Coleman, J.T.	82	Hung, C.C.	76
Coles, W.A.	92	Iizuka, K.	10, 24
Collins, R.E.	81	Ing, D.R.	97
Connold, D.M.	48	Ishimaru, A.	95
Cooper, S.E.	55	Kalhor, H.A.	76, 94
Cowan, W.M.	15	Katz, A.H.	62
Cox, D.C.	17	Katz, I.	32
Crane, R.K.	33, 34, 36	Kendall, B.R.	76
Cubley, D.H.	4	Klobuchar, J.F.	42
Cummins, J.A.	55	Kreiss, A.D.	76
Daley, J.C.	23	Kummer, W.H.	27
DaRosa, A.V.	58	Kuo, N.H.	93

Lake, H.	27, 37	Rush, C.M.	63
Lamb, J.J.	29	Sanderson, A.E.	7
Lammers, U.H.W.	19	Scherer, J.P.	76
Lawton, R.A.	10	Schmid, H.F.	21
Lee, H.S.	60	Schroeder, K.G.	88
Levis, C.A.	3	Sengupta, P.R.	56, 58, 59
Lindsey, J.F. III	4	Sherman, S.M.	53
Lo, Y.T.	77, 90	Silver, S.	35
Lorentzen, A.H.	86	Shmoys, J.	48
Lyon, G.F.	42	Shomo, A.P.	76
Lyons, L.	63	Slack, F.F.	42
Lyons, L.A.	3	Soicher, H.	62
McClure, J.P.	68	Steinberg, B.D.	54
McCormick, K.S.	19	Straiton, A.W.	35
Miles, M.J.	21	Strickland, J.I.	37
Miller, E.	5	Sweeny, L.E. Jr.	8
Mills, R.	6	Thome, G.D.	43, 44
Miner, G.	35	Thomson, D.W.	16
Mittra, R.	77	Tischer, F.J.	98
Mitzner, K.M.	75	Toman, K.	86
Moo, C.A.	52	Tong, T.C.H.	76
Nagelberg, E.R.	90	Tsao, C.K.H.	67
Neureuther, A.R.	76, 94	Tseng, F-I	96
Nisbet, J.S.	69	Ulaby, F.T.	35
Norair, N.	75	Underwood, J.S.	67
Ottersten, H.	32	VanZandt, T.E.	68
Patton, D.E.	44	Wagner, L.S.	58
Penndorf, R.	65	Wagner, R.A.	60
Perry, B.D.	66	Wait, D.F.	9
Peterson, V.L.	68	Warner, R.	69
Pike, C.P. Jr.	63	Washburn, T.W.	54, 55
Pjerron, G.	5	Waterman, A.T. Jr.	17, 26
Plonus, M.A.	93	Watkins, S.N.	18
Poeverlein, H.	49	Weil, H.	84
Pollon, G.E.	5	Welch, W.J.	35, 92
Potter, W.H.	84	Whalen, J.	65
Randall, D.	32	Wilson, C.	44
Rao, B.R.	83	Wilson, R.W.	36
Rao, K.M.	38	Wu, C.P.	93
Rao, N.N.	42, 64	Yeh, C.	85
Rao, P.B.	43	Yeh, K.C.	49
Reid, G.C.	59	Yorks, R.G.	84
Roche, J.F.	27, 67	Youakim, M.Y.	64
Rogers, R.R.	38	Young, G.O.	27
Rouffy, F.	88	Zimmerman, M.S.	54
Rumsey, V.H.	92	Zimmerman, S.P.	47
Ruscio, J.T.	36	Zolnay, S.L.	3, 18









1969 USNC-URSI SPRING MEETING

22-25 April

Washington, D.C.

1969 URSI GENERAL ASSEMBLY

18-29 August

Canada

1969 USNC-URSI FALL MEETING

9-12 December

University of Texas
Austin, Texas

1969 Fall URSI Meeting - Local Steering Committee

E.E. Altshuler
P. Blacksmith
P.C. Fritsch
D.L. Fye
M. Loewenthal

R.B. Mack
H.R. Raemer
L.J. Ricardi
C.J. Sletten

THIS COPY BELONGS TO:

Name _____

Company _____

Address _____

If found return to above or

Northeastern University, Room 112H.